

6/8/81
COPY 1 2

MICROWAVE LANDING SYSTEM FLARE SUBSYSTEM TEST

Carl B. Jezierski

FEDERAL AVIATION ADMINISTRATION

NOV 2 1981

TECHNICAL CENTER LIBRARY
ATLANTIC CITY, N.J. 08405

FEDERAL AVIATION ADMINISTRATION TECHNICAL CENTER
Atlantic City Airport, New Jersey 08405



DATA REPORT

OCTOBER 1981

Document is available to the U.S. public through
the National Technical Information Service,
Springfield, Virginia 22161.

Prepared for

**U. S. DEPARTMENT OF TRANSPORTATION
FEDERAL AVIATION ADMINISTRATION
Systems Research & Development Service
Washington, D. C. 20590**

FAA TECHNICAL CENTER LIBRARY NJ

United State/Microwave landing system fl



00007543

NOTICE

This document is disseminated under the sponsorship of the Department of Transportation in the interest of information exchange. The United States Government assumes no liability for the contents or use thereof.

The United States Government does not endorse products or manufacturers. Trade or manufacturer's names appear herein solely because they are considered essential to the object of this report.

Technical Report Documentation Page

1. Report No. FAA-CT-81-61		2. Government Accession No.		3. Recipient's Catalog No.	
4. Title and Subtitle MICROWAVE LANDING SYSTEM FLARE SUBSYSTEM TEST				5. Report Date October 1981	
				6. Performing Organization Code ACT-100	
7. Author(s) Carl B. Jezierski				8. Performing Organization Report No. FAA-CT-81-61	
9. Performing Organization Name and Address Federal Aviation Administration Technical Center Atlantic City Airport, New Jersey 08405				10. Work Unit No. (TRAIS)	
				11. Contract or Grant No. 075-725-420	
12. Sponsoring Agency Name and Address Federal Aviation Administration Technical Center Atlantic City Airport, New Jersey 08405				13. Type of Report and Period Covered Data Report April 1979	
				14. Sponsoring Agency Code	
15. Supplementary Notes					
16. Abstract Microwave Landing System (MLS) Flare subsystem performance data were collected on a specially instrumented Federal Aviation Administration (FAA) Technical Center aircraft. The airborne data were compared with a theodolite tracking system reference and error plots generated. Due to extensive lightning damage only two flight tests were performed. Flare subsystem accuracy could not be determined because of insufficient data.					
17. Key Words MLS Flare Subsystem			18. Distribution Statement Document is available to the U.S. public through the National Technical Information Service, Springfield, Virginia 22161		
19. Security Classif. (of this report) Unclassified		20. Security Classif. (of this page) Unclassified		21. No. of Pages 45	22. Price

METRIC CONVERSION FACTORS

Approximate Conversions to Metric Measures

Symbol	When You Know	Multiply by	To Find	Symbol
LENGTH				
in	inches	*2.5	centimeters	cm
ft	feet	30	centimeters	cm
yd	yards	0.9	meters	m
mi	miles	1.6	kilometers	km
AREA				
in ²	square inches	6.5	square centimeters	cm ²
ft ²	square feet	0.09	square meters	m ²
yd ²	square yards	0.8	square meters	m ²
mi ²	square miles	2.6	square kilometers	km ²
	acres	0.4	hectares	ha
MASS (weight)				
oz	ounces	28	grams	g
lb	pounds	0.45	kilograms	kg
	short tons (2000 lb)	0.9	tonnes	t
VOLUME				
tsp	teaspoons	5	milliliters	ml
Tbsp	tablespoons	15	milliliters	ml
fl oz	fluid ounces	30	milliliters	ml
c	cups	0.24	liters	l
pt	pints	0.47	liters	l
qt	quarts	0.95	liters	l
gal	gallons	3.8	liters	l
ft ³	cubic feet	0.03	cubic meters	m ³
yd ³	cubic yards	0.76	cubic meters	m ³
TEMPERATURE (exact)				
°F	Fahrenheit temperature	5/9 (after subtracting 32)	Celsius temperature	°C

*1 in = 2.54 (exactly). For other exact conversions and more detailed tables, see NBS Misc. Publ. 286, Units of Weights and Measures, Price \$2.25, SD Catalog No. C13.10:286.



Approximate Conversions from Metric Measures

Symbol	When You Know	Multiply by	To Find	Symbol
LENGTH				
mm	millimeters	0.04	inches	in
cm	centimeters	0.4	inches	in
m	meters	3.3	feet	ft
m	meters	1.1	yards	yd
km	kilometers	0.6	miles	mi
AREA				
cm ²	square centimeters	0.16	square inches	in ²
m ²	square meters	1.2	square yards	yd ²
km ²	square kilometers	0.4	square miles	mi ²
ha	hectares (10,000 m ²)	2.5	acres	
MASS (weight)				
g	grams	0.035	ounces	oz
kg	kilograms	2.2	pounds	lb
t	tonnes (1000 kg)	1.1	short tons	
VOLUME				
ml	milliliters	0.03	fluid ounces	fl oz
l	liters	2.1	pints	pt
l	liters	1.06	quarts	qt
l	liters	0.26	gallons	gal
m ³	cubic meters	35	cubic feet	ft ³
m ³	cubic meters	1.3	cubic yards	yd ³
TEMPERATURE (exact)				
°C	Celsius temperature	9/5 (then add 32)	Fahrenheit temperature	°F

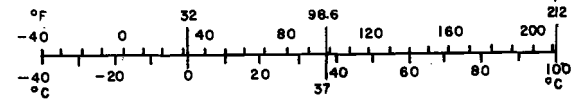


TABLE OF CONTENTS

	Page
INTRODUCTION	1
Purpose	1
Background	1
DATA COLLECTION	1
DATA REDUCTION AND ANALYSIS	3
Raw Error Data	3
Diagnostic Data	3
Path Following Error	6
Control Motion Noise	8
REFERENCES	8
APPENDICES	
A — Raw Error Plots	
B — Diagnostic Plots	
C — Expanded Raw and Path Following Error Plots	
D — Control Motion Noise Plots	

LIST OF ILLUSTRATIONS

Figure		Page
1	Airborne Data Acquisition Instrumentation	2
2	Test Bed MLS Subsystems and Tracking Sites	2
3	Flight Profiles	4
4	Airborne Data Filter Algorithm Flow Chart	5
5	MLS Flare Data Processing Flow Diagram	6

LIST OF TABLES

Table		Page
1	Test Bed MLS Siting Constants	1
2	Aircraft Tracking Cross Offsets	7

INTRODUCTION

PURPOSE.

The objective of this project was to evaluate performance of the Microwave Landing System (MLS) Flare subsystem.

BACKGROUND.

The Flare subsystem supplies uninterrupted elevation guidance during the flareout under Category-3 weather minimums after the aircraft has flown past the normal MLS elevation coverage zone (typically, the runway threshold). The Flare subsystem, designed and constructed in Australia, was integrated into the MLS test bed facility on runway 31 at the Federal Aviation Administration (FAA) Technical Center to support continuing development of the flare function.

DATA COLLECTION

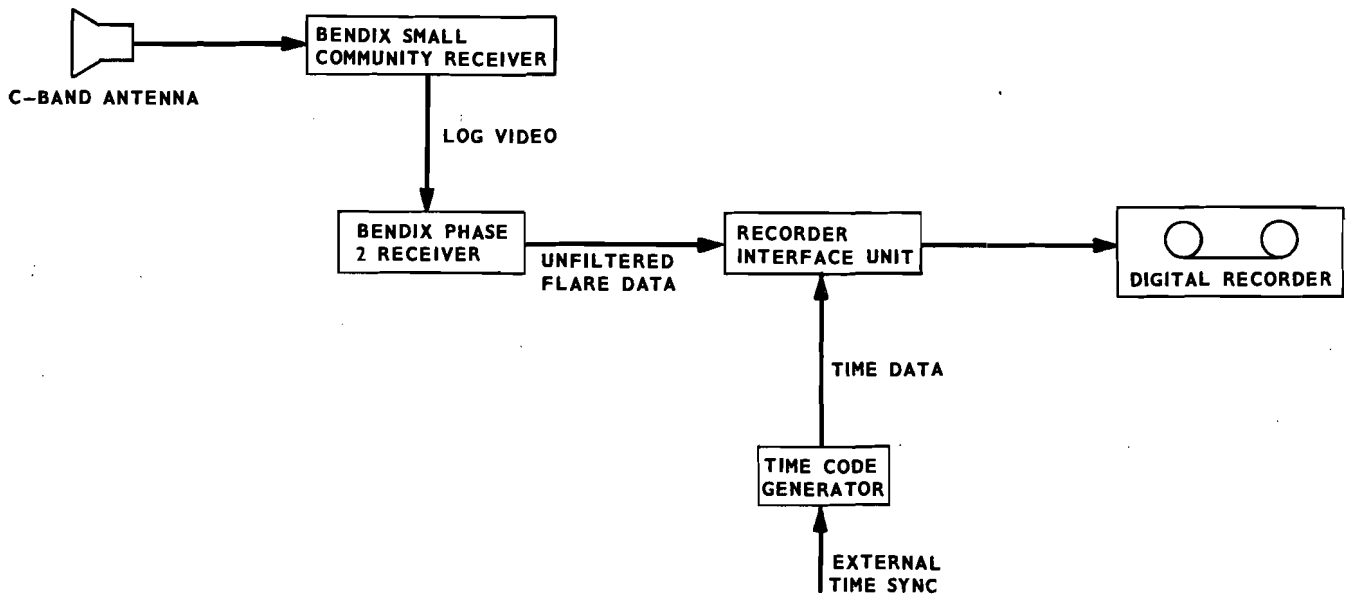
The FAA Technical Center's Aerocommander aircraft, N-50, was instrumented to collect the airborne flare data (figure 1). A C-band omnidirectional antenna, installed between the aircraft nose and the wind screen base, received and fed the MLS guidance signals to a Bendix Small Community (SC) receiver that produced a log video output signal. The log video was then fed to a Bendix phase-2 receiver which decoded the flare function and produced the digital flare angle data. Two receivers were used because the SC receiver was not configured to decode the flare information and the phase-2 receiver could not process the raw radiofrequency (RF) signal.

The digital output from the phase-2 receiver was then fed to the recorder interface unit, tagged with time information, and formatted for recording on 9-track digital tape.

The aircraft was tracked by the theodolite tracking system located at the Technical Center. Figure 2 shows the layout of the MLS subsystems and the theodolite tracking towers. MLS siting constants obtained from precise surveys are listed in table 1.

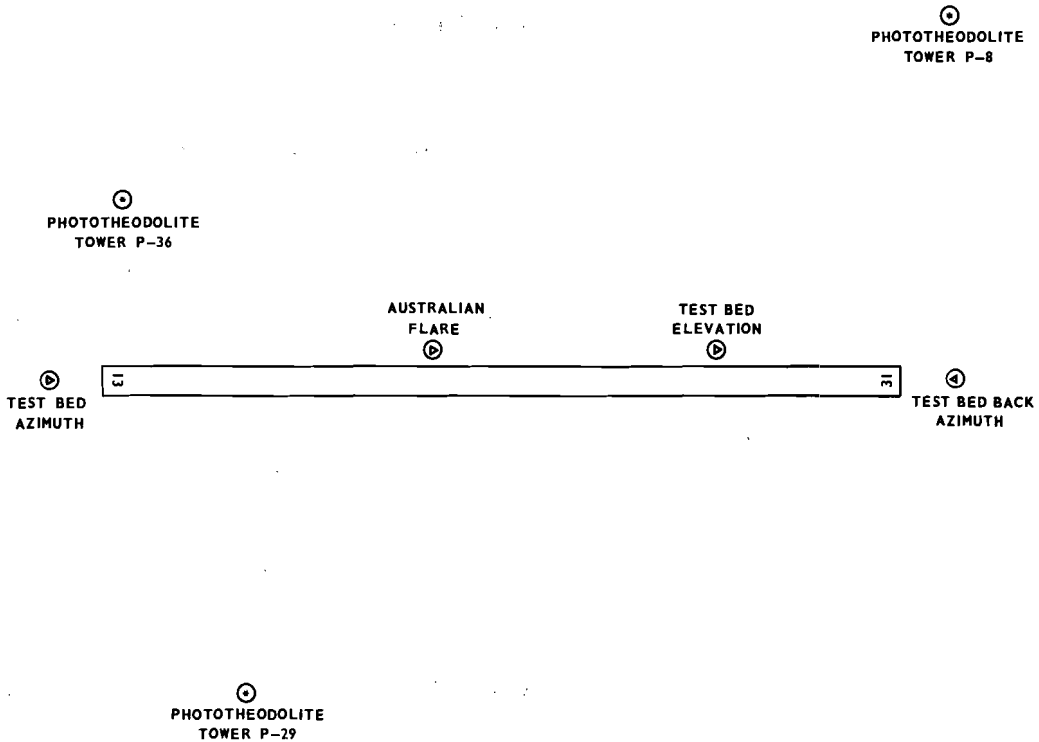
TABLE 1. TEST BED MLS SITING CONSTANTS

<u>Site</u>	<u>(Feet)</u>		
	<u>X</u>	<u>Y</u>	<u>Z</u>
Azimuth Phase Center	0.0	0.0	0.0
Elevation Phase Center	9,730.78	429.03	-14.67
Flare Phase Center	7,312.73	431.10	-7.16
Back Azimuth Phase Center	11,362.82	0.26	-12.11
Threshold (Runway 31)	10,781.87	0.0	



81-61-1

FIGURE 1. AIRBORNE DATA ACQUISITION INSTRUMENTATION



81-61-2

FIGURE 2. TEST BED MLS SUBSYSTEMS AND TRACKING SITES

Flare subsystem operation was checked prior to flight testing using an instrumented test van. The results indicated normal operation and the first of two flight profiles (figure 3) was flown the following day.

A series of five approaches were flown to runway 31 using front azimuth and flare guidance (April 11, 1979, odd numbered runs). Excessive shadowing by the aircraft's fuselage rendered data collected on the return trips useless. Hence, no even-numbered runs are included in this report. The second flight profile consisted of six partial orbits at an altitude of 1,700-feet and 4 nautical miles (nmi) from the field distance measuring equipment (DME) site for a flare elevation angle of approximately 4°. Only five runs were processed because tracking data for the first run were lost. Recorded data from these runs indicated normal operation without anomalies in the coverage region. Extensive lightning damage to the flare antenna electronics precluded further flight testing.

DATA REDUCTION AND ANALYSIS

The airborne data were filtered before merging with the tracker information employing an MLS Phase-2 receiver filter algorithm. It consists of an angle slew rate limiter, driving a single pole, low-pass digital filter and was implemented on a General Automation GA-16/440 minicomputer. A flow chart representation of the algorithm is shown in figure 4.

After the filtering operation, the airborne data were time correlated (merged) with the magnetic tape tracking data on the Technical Center's Honeywell 66/60 computer. The merge operation provided a data base on tape for plotting and future processing, and a disk file for immediate analysis on a remote graphics terminal. The flare data processing flow diagram is shown in figure 5.

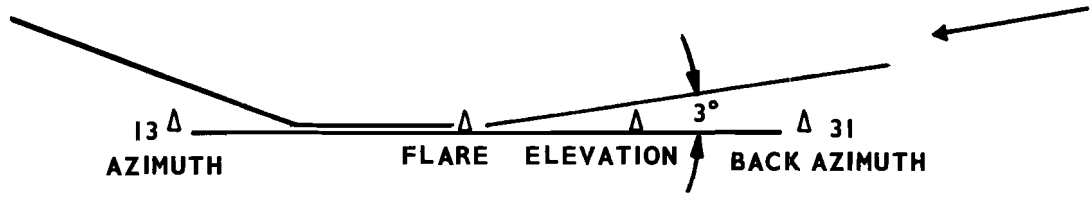
Four different output plots were generated as follows: (1) raw error plots for centerline approaches and partial orbits, (2) diagnostic plots showing filtered receiver output angle data and tracker derived angle data for centerline approaches, (3) path following error (PFE) filtered data, and (4) control motion noise (CMN) filtered data.

RAW ERROR DATA.

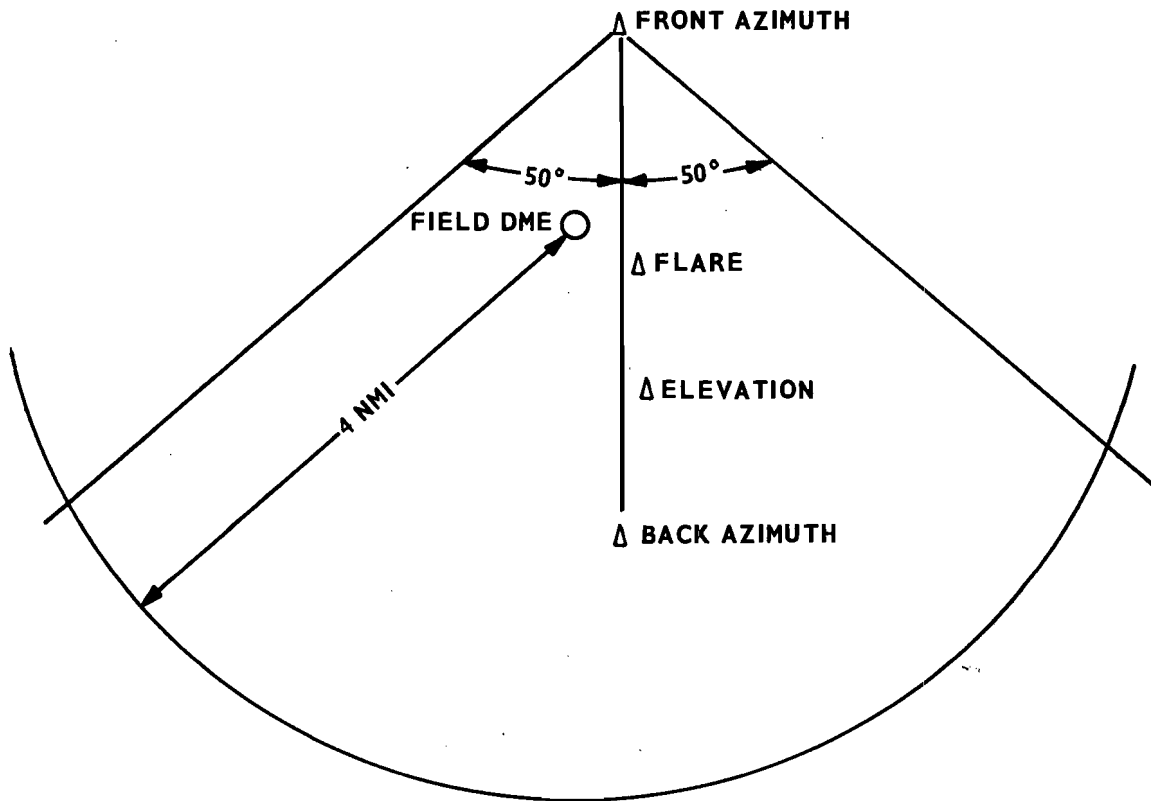
The raw error plots in appendix A show the difference between the receiver angle and the actual angle derived from the ground tracker data and are used to check coverage regions. The 3° centerline approach error plots (figures A-1 through A-5, appendix A) indicate that proportional guidance was provided in the region 2,500 feet inside threshold (1.36 nmi from azimuth phase center) to beyond 5 nmi from threshold. The partial orbit error plots (figures A-6 through A-10, appendix A) show that proportional guidance is provided in an azimuth sector well exceeding $\pm 10^\circ$ about the runway centerline.

DIAGNOSTIC DATA.

The diagnostic plots in appendix B show the receiver angle data and tracker information used in calculating the error plots. These plots are used only to help identify the source of sudden variations in the corresponding error plots. The



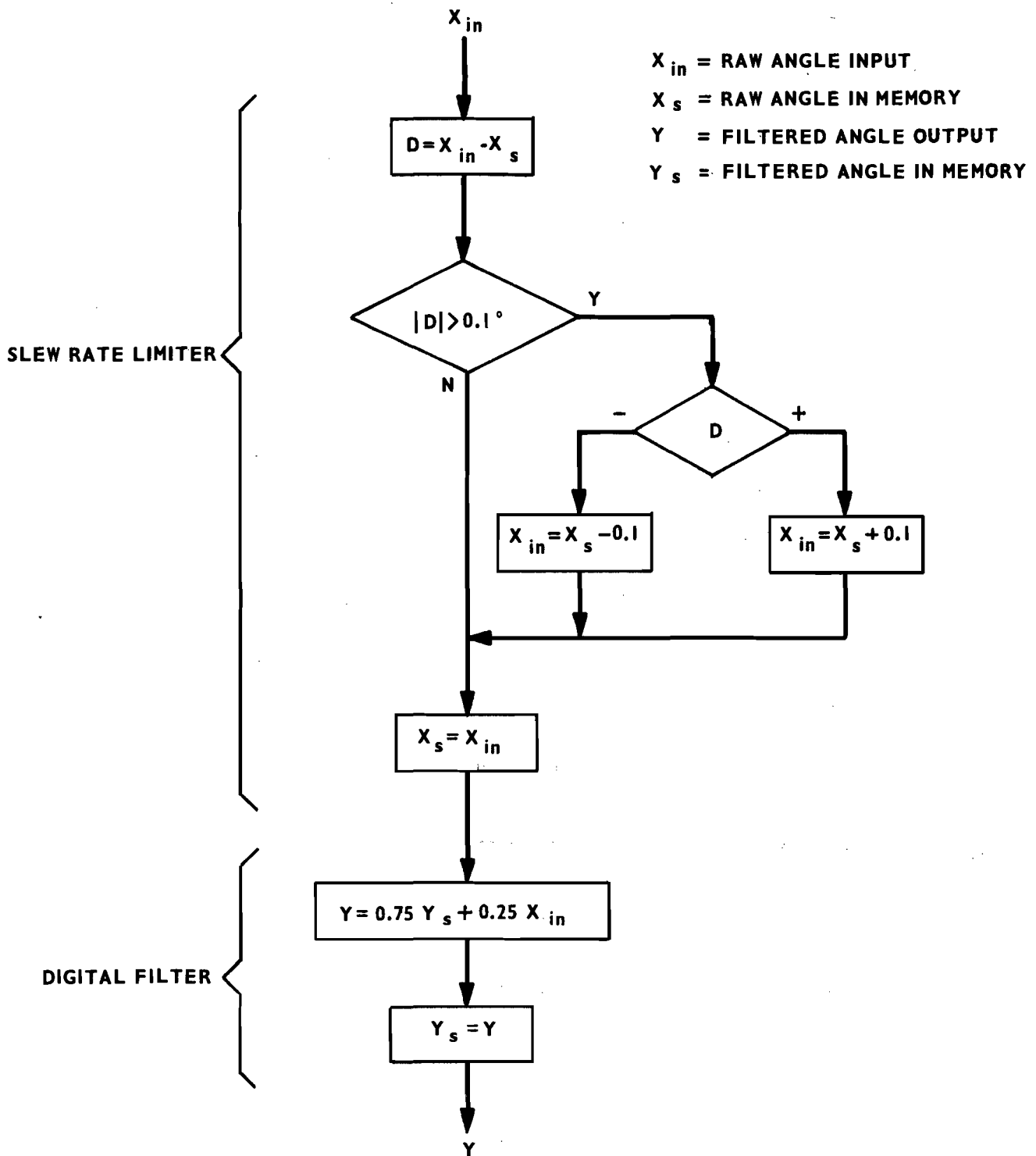
PROFILE 1 CENTERLINE, 3° GLIDESLOPE APPROACH
(NOT TO SCALE)



PROFILE 2 PARTIAL ORBITS, 1700 FEET ALTITUDE
(NOT TO SCALE)

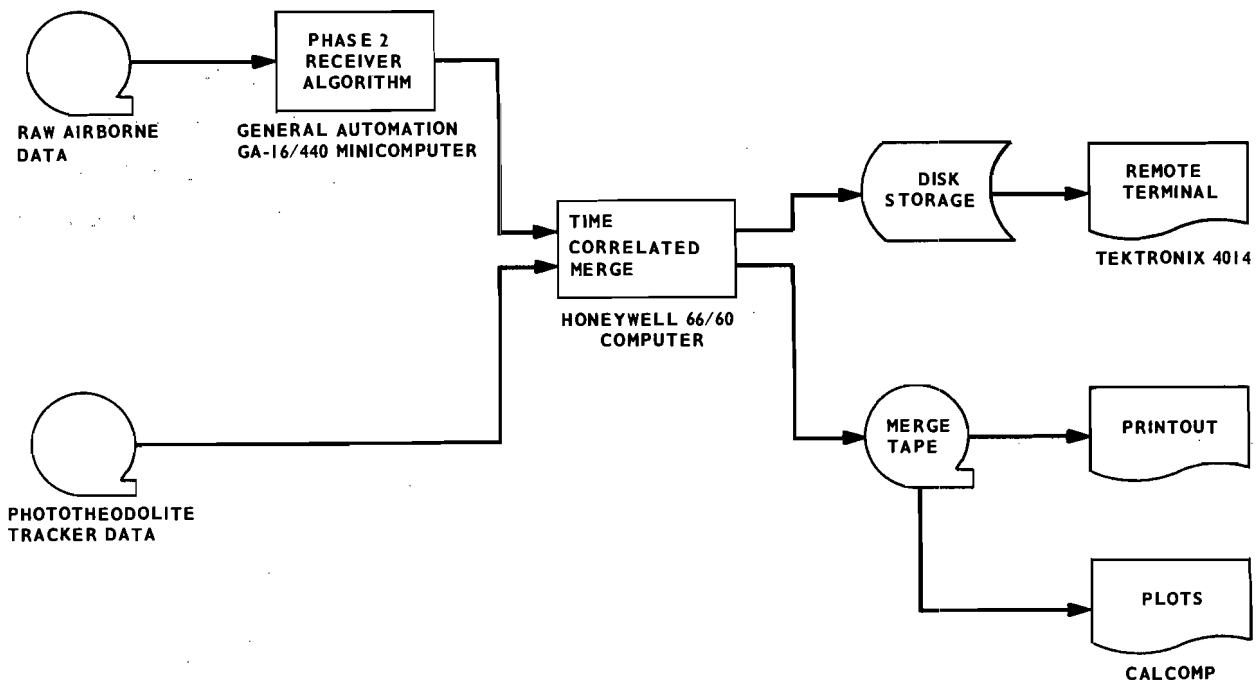
81-61-3

FIGURE 3. FLIGHT PROFILES



81-61-4

FIGURE 4. AIRBORNE DATA FILTER ALGORITHM FLOW CHART



81-61-5

FIGURE 5. MLS FLARE DATA PROCESSING FLOW DIAGRAM

diagnostic plots, figures B-1 through B-5, correspond to the error plots, figures A-1 through A-5, respectively. Diagnostic plots are not provided for the partial orbit flight profiles because the scale factor required to cover a $\pm 10^\circ$ sector rendered the receiver and tracker traces indistinguishable from each other.

PATH FOLLOWING ERROR.

The graphs in appendix C show the angular and linear PFE characteristics in the region of interest. PFE is defined as the theoretical worst case deviation from a preselected course of an aircraft following MLS guidance commands and is estimated using a filter with the following transfer function obtained from reference 1:

$$H(s) = \frac{\omega_n^2}{s^2 + 2\omega_n s + \omega_n^2}; \omega_n = 3.13 \text{ radians/second} \quad (1)$$

The region of interest is that section of runway 31 between 300 and 2,800 feet inside threshold where the flare accuracy should be comparable to that of radio altimeters. A bias of 0.05° , calculated from the raw error data in this region, was subtracted from the raw error rather than adjusting the mechanical tilt of the flare antenna and electrical bias within the flare antenna driver and cabling. The

raw error with bias removed (θ_{err}) is plotted as raw angular error in figures C-1 through C-5. θ_{err} was passed through a digital filter which implemented the transfer function of equation (1) and is shown as PFE filtered angular error in plots C-1 through C-5.

Linear vertical error was obtained from θ_{err} and range. A precision DME receiver would normally provide range data, but the theodolite tracker data was employed to obtain independent flare subsystem errors. Using the tracker, ground range (R_g) was calculated as follows:

$$R_g = \sqrt{(X_t - X_{fl} - P_x)^2 + (Y_t - Y_{fl} - P_y)^2} \quad (2)$$

where:

X_t, Y_t = target coordinates recorded by tracker

X_{fl}, Y_{fl} = flare antenna phase center coordinates

P_x, P_y = tracking cross offsets from the MLS receiving antenna

Tracking cross offset constants are given in table 2. Vertical error (E_v) was then calculated as:

$$E_v = (R_g)\tan(\theta_{err}) \quad (3)$$

and is plotted as raw linear error in figures C-1 through C-5. The PFE filtered angular error was substituted for θ_{err} in equation (3) and the resulting E_v was plotted as PFE filtered linear error in figures C-1 through C-5.

TABLE 2. AIRCRAFT TRACKING CROSS OFFSETS

$P_x = 2.583$ feet

$P_y = 0.000$ feet

$P_z = 0.667$ feet

PFE tolerance limits of ± 2 feet, as defined by the December 22, 1980 draft MLS Standards and Recommended Practices (SARPS), are superimposed upon both the angular and linear filtered error plots as an aid to evaluation. Examination of the PFE filtered linear error plots from the five available runs reveals that the error marginally exceeds the tolerance limits between -300 and -1,500 feet from threshold. On runs 1 and 3 (figures C-1 and C-2) the error increases rapidly between -2,500 and -2,800 feet from threshold. It should be noted that inside this region, the flare angle changes rapidly and theodolite tracking degrades because theodolite station P8 can no longer "see" the aircraft tracking point (figure 2). Only real-time magnetic tape data (not film corrected data) were used because film reading equipment was not available. Film data are used to correct operator

tracking errors for greater accuracy. Two-sigma tracking accuracy of real time magnetic tape data is specified in reference 2 as ± 1.5 feet in the z-axis and ± 2 feet in the x- and y-axes.

Because of the limited number of error plots available for analysis and the lack of film-corrected tracking data, flare antenna PFE accuracy could not be determined.

CONTROL MOTION NOISE.

The angular and linear CMN error plots for the region of interest are shown in appendix D.

CMN is noise which causes control surface, column and wheel motion, but does not significantly affect aircraft position. CMN is estimated by using a bandpass filter with the following transfer function obtained from reference 1:

$$H(s) = \left(\frac{s}{s + \omega_1} \right) \left(\frac{\omega_2}{s + \omega_2} \right); \quad \begin{array}{l} \omega_1 = 0.5 \text{ radians/second} \\ \omega_2 = 10.0 \text{ radians/second} \end{array} \quad (4)$$

θ_{err} was passed through a digital filter implementing the transfer function of equation (4). The output of this operation is the angular control motion noise and is plotted in figures D-1 through D-5 (appendix D). The vertical error was calculated by substituting the angular control motion noise data for θ_{err} in equation (3) and is shown in figures D-1 through D-5. Both linear and angular CMN plots were generated because the MLS SARPS specifies a linear tolerance (± 1 foot) and an angular tolerance ($\pm 0.07^\circ$) for CMN.

Examination of the linear CMN plots in appendix D shows that the errors exceed the ± 1 -foot tolerance well beyond the allowable 5 percent limit over a 10-second evaluation interval. The errors are not consistent as a function of range and do not follow an obvious trend. More precise tracker data are required to evaluate a system that has a ± 1 -foot accuracy specification.

The angular CMN plots in appendix D are generally within the specified $\pm 0.07^\circ$ tolerance except between $-2,400$ and $-2,800$ feet from threshold. However, it should be noted that in this region a tracking error of 1.5 feet in the z-axis results in a flare angular error of 0.11° at $-2,800$ feet from threshold. The explanation of theodolite tracking accuracy, previously given in the "Path Following Error" section, also applies to CMN.

Because of the limited number of error plots available for analysis and the lack of film-corrected tracking data, flare antenna CMN accuracy could not be determined.

REFERENCES

1. ICAO Test Plan for U.S. Microwave Landing System, Department of Transportation, Federal Aviation Administration, March 31, 1975.
2. Microwave Landing System Phase II Tracker Error Study, Federal Aviation Administration, Report No. FAA-RD-74-207, December 1974.

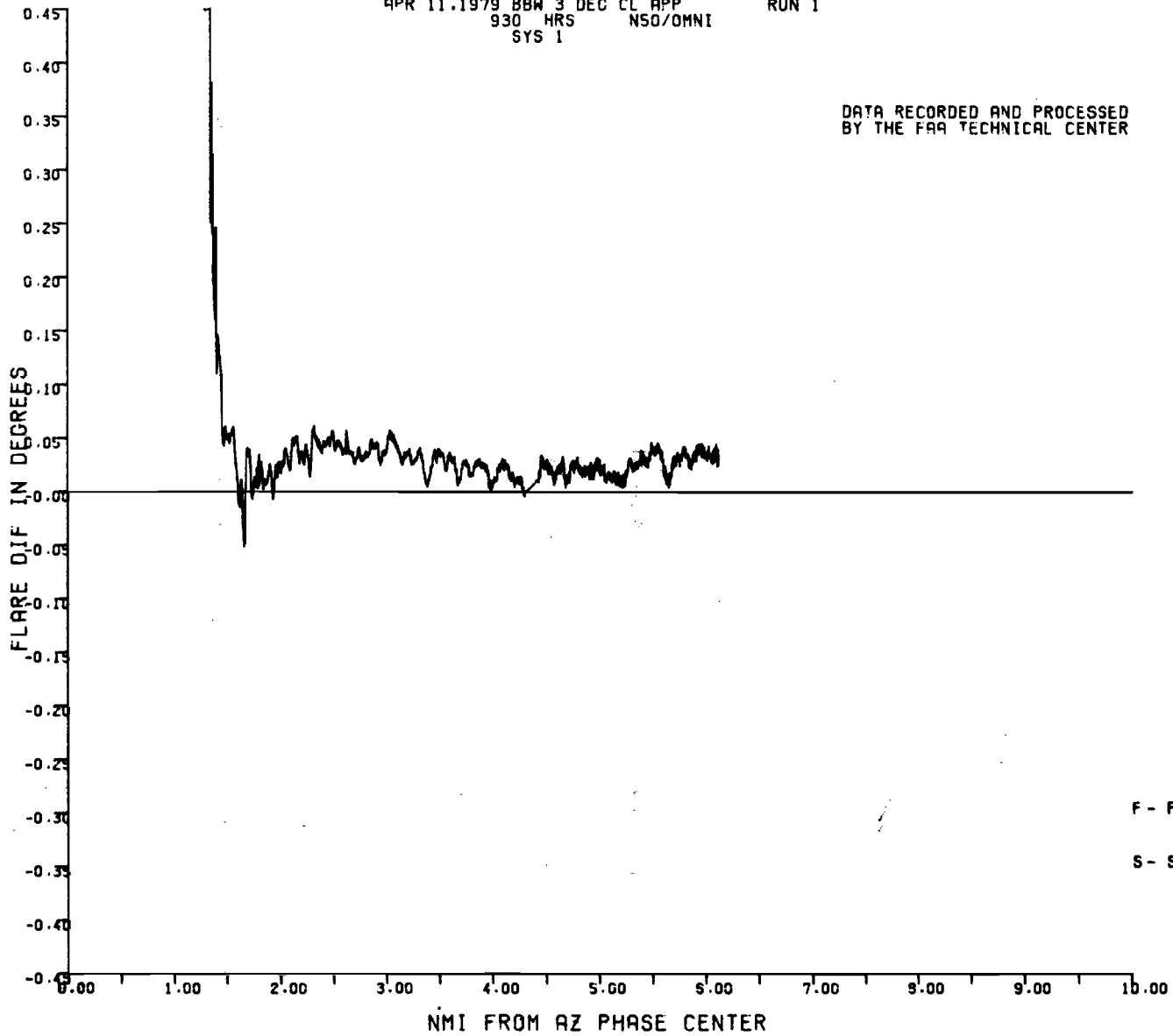
APPENDIX A
RAW ERROR PLOTS

<u>Type of Pattern</u>	<u>Page No.</u>
3° glide slope, centerline	A-1 to A-5
Partial orbit at 4 nmi and 1,700-foot altitude	A-6 to A-10

A-1

APR 11.1979 BBW 3 DEC CL APP RUN 1
930 HRS NSO/OMNI
SYS 1

DATA RECORDED AND PROCESSED
BY THE FAA TECHNICAL CENTER



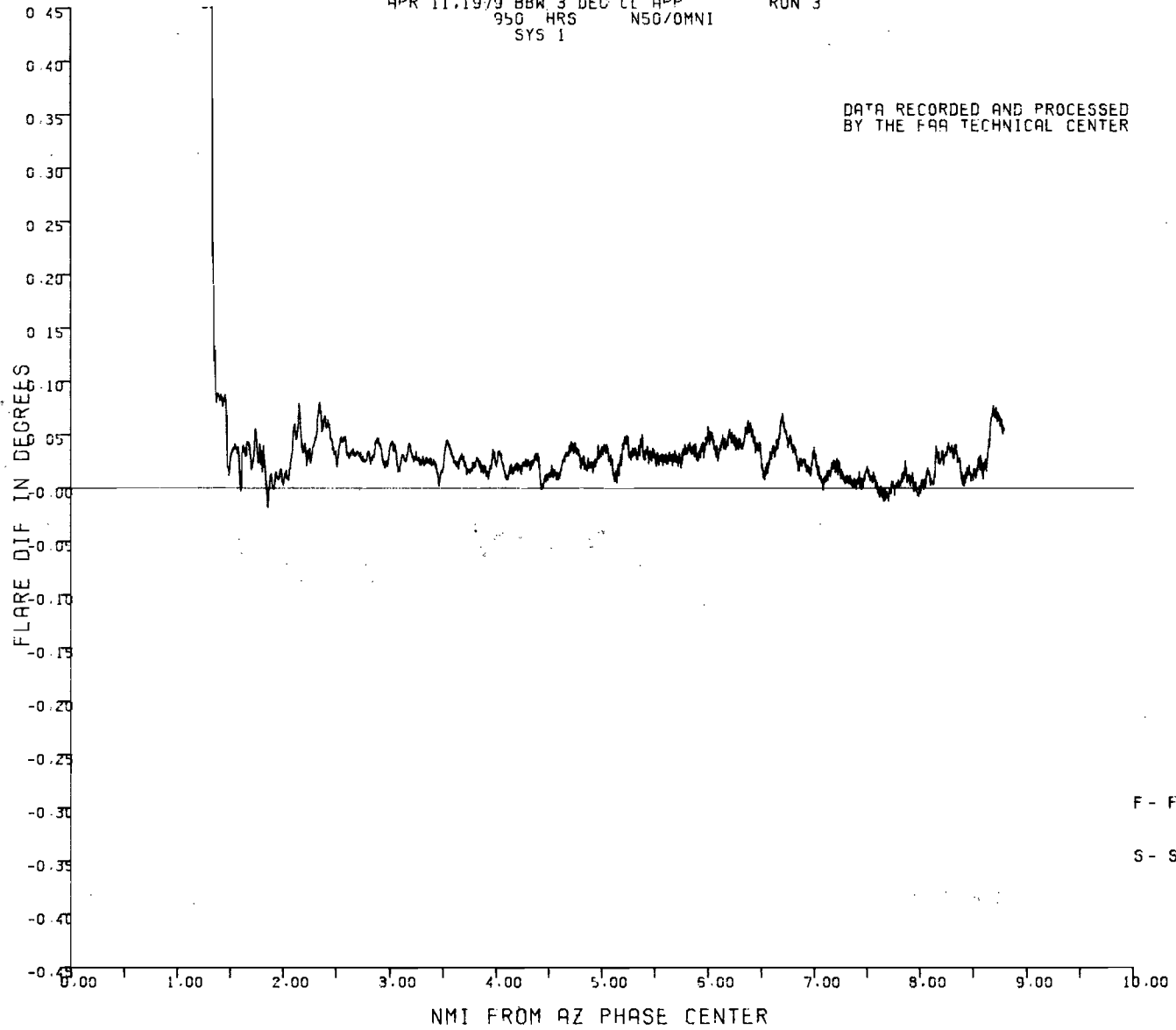
F - FRAME FLAG

S - SYSTEM FLAG

81-61-A-1

APR 11, 1979 BBW 3 DEC CL APP RUN 3
950 HRS N50/OMNI
SYS 1

DATA RECORDED AND PROCESSED
BY THE FAA TECHNICAL CENTER



F - FRAME FLAG

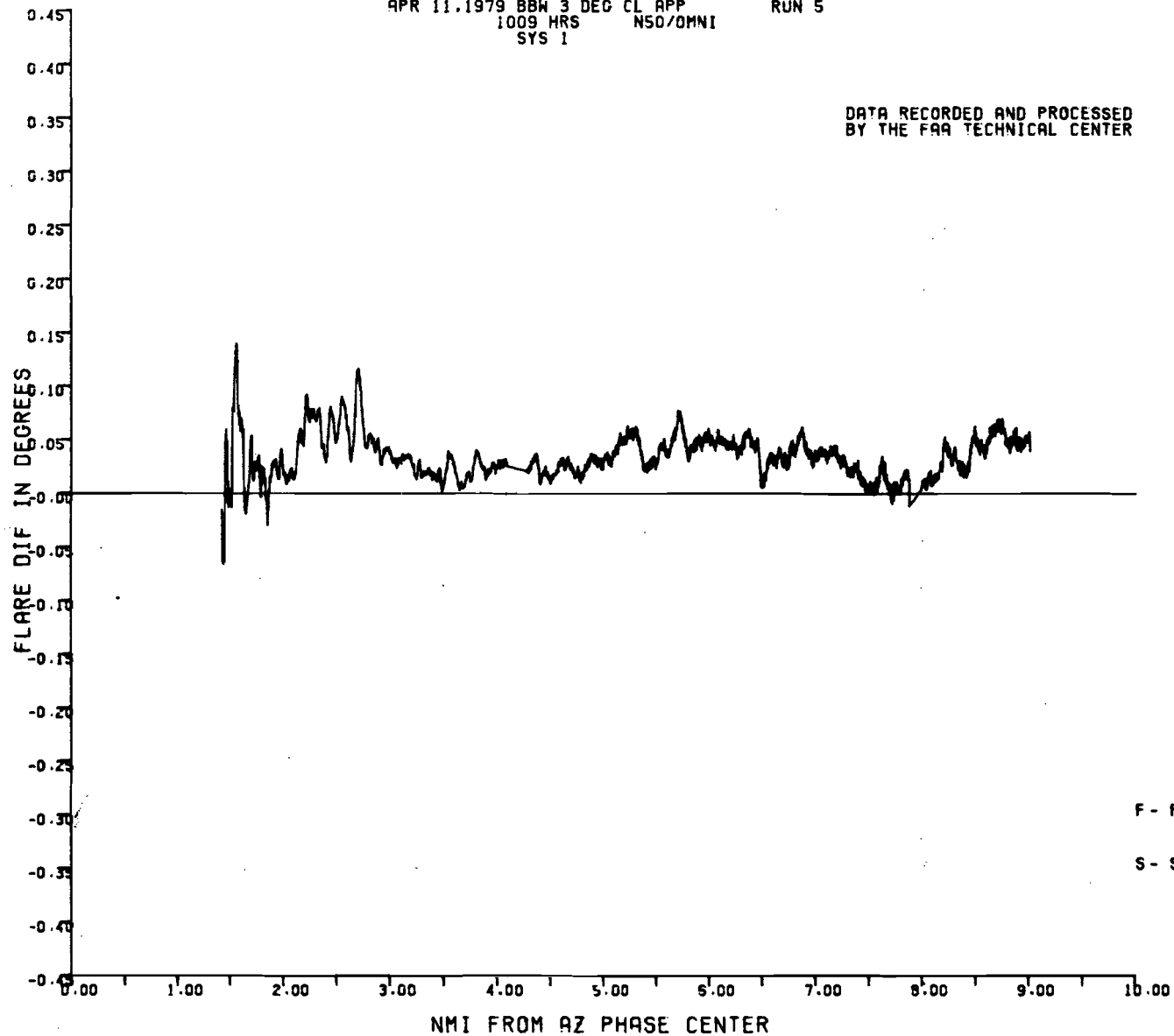
S - SYSTEM FLAG

A-2

81-61-A-2

APR 11.1979 BBW 3 DEG CL APP RUN 5
1009 HRS NSD/OMNI
SYS 1

DATA RECORDED AND PROCESSED
BY THE FAA TECHNICAL CENTER

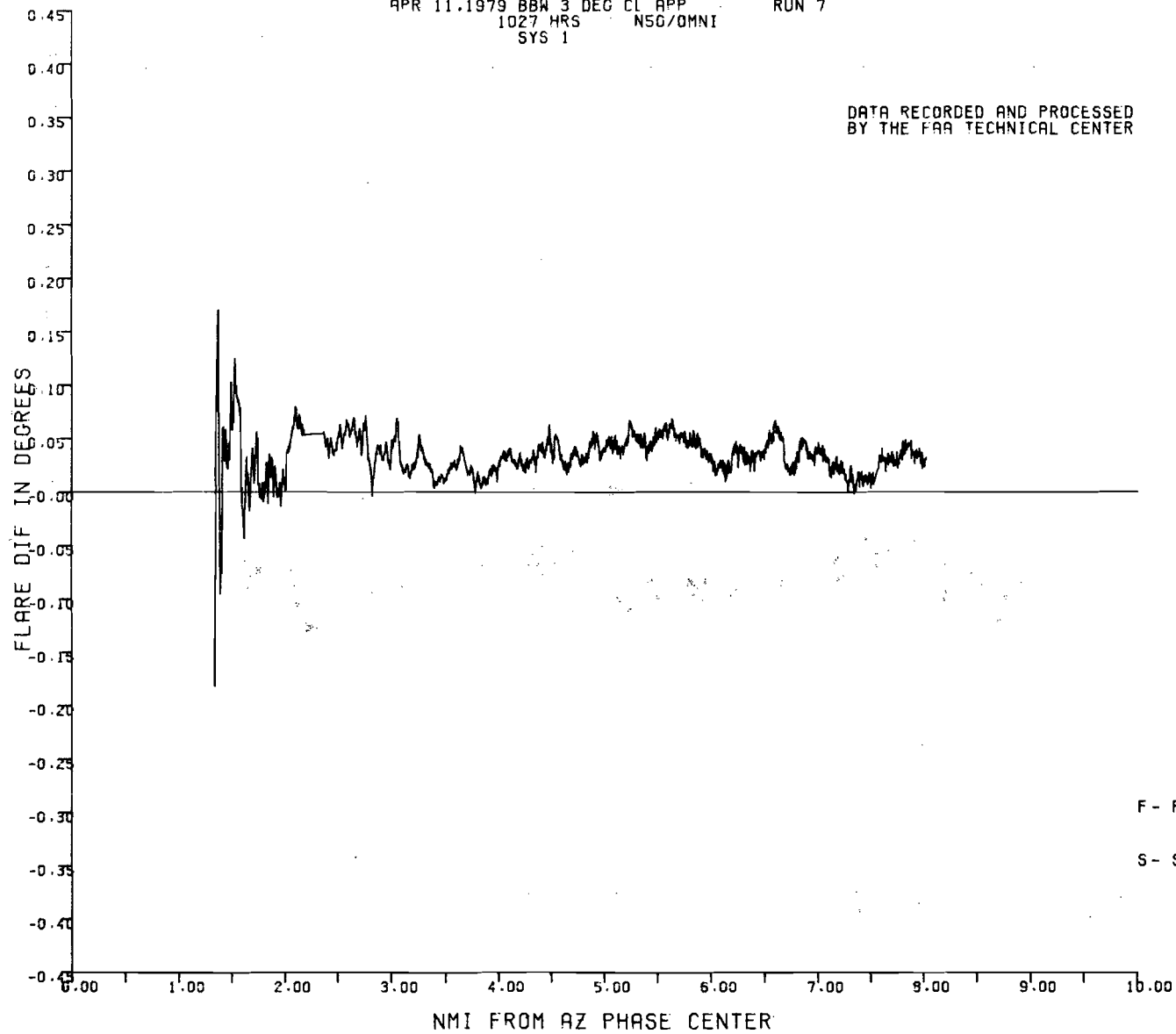


F - FRAME FLAG
S - SYSTEM FLAG

A-3

APR 11.1979 BBW 3 DEG CL APP RUN 7
1027 HRS NSG/OMNI
SYS 1

DATA RECORDED AND PROCESSED
BY THE FAA TECHNICAL CENTER



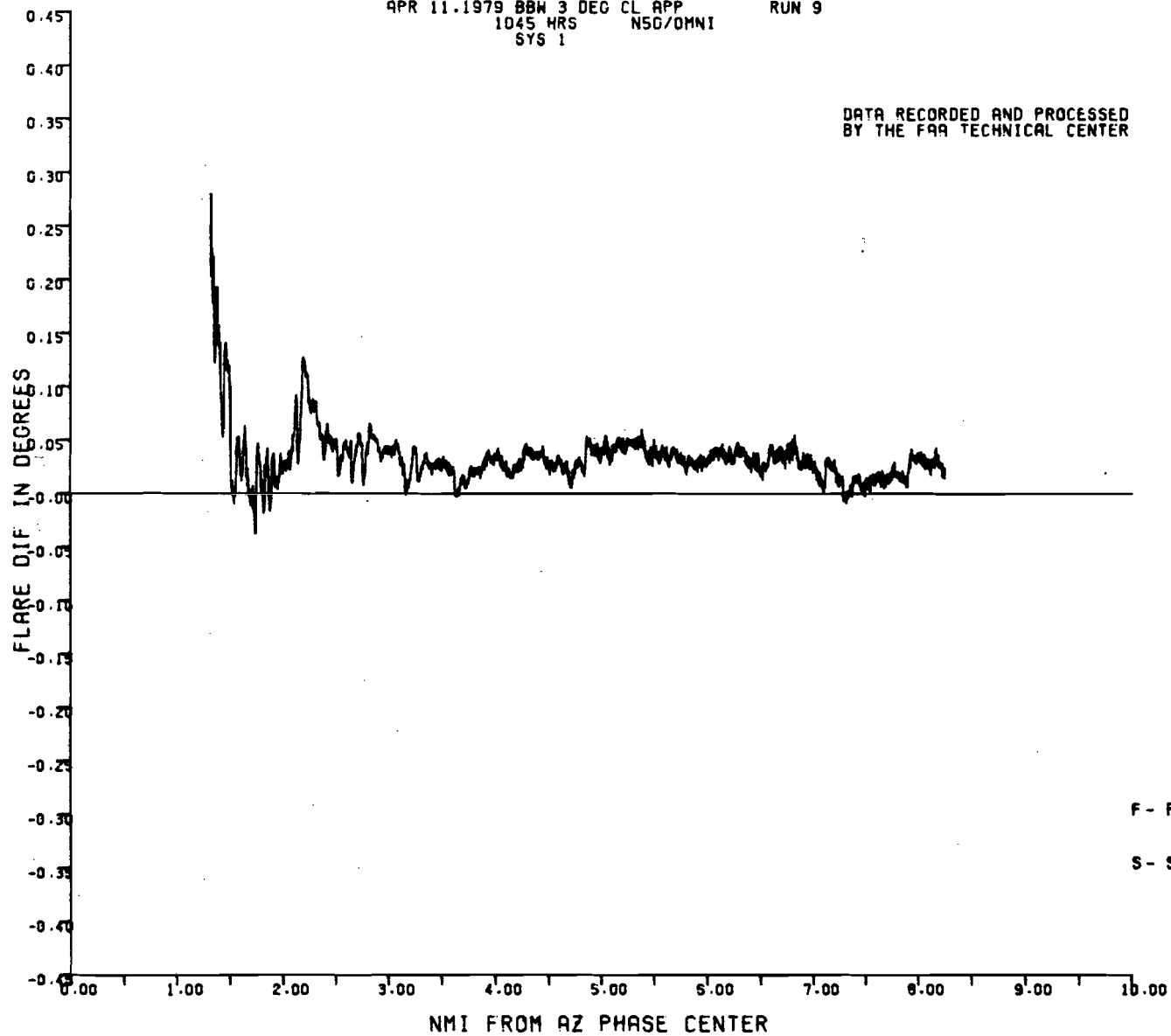
F - FRAME FLAG
S - SYSTEM FLAG

A-4

81-61-A-4

APR 11.1979 BBW 3 DEG CL APP RUN 9
1045 HRS NSD/OMNI
SYS 1

DATA RECORDED AND PROCESSED
BY THE FAA TECHNICAL CENTER



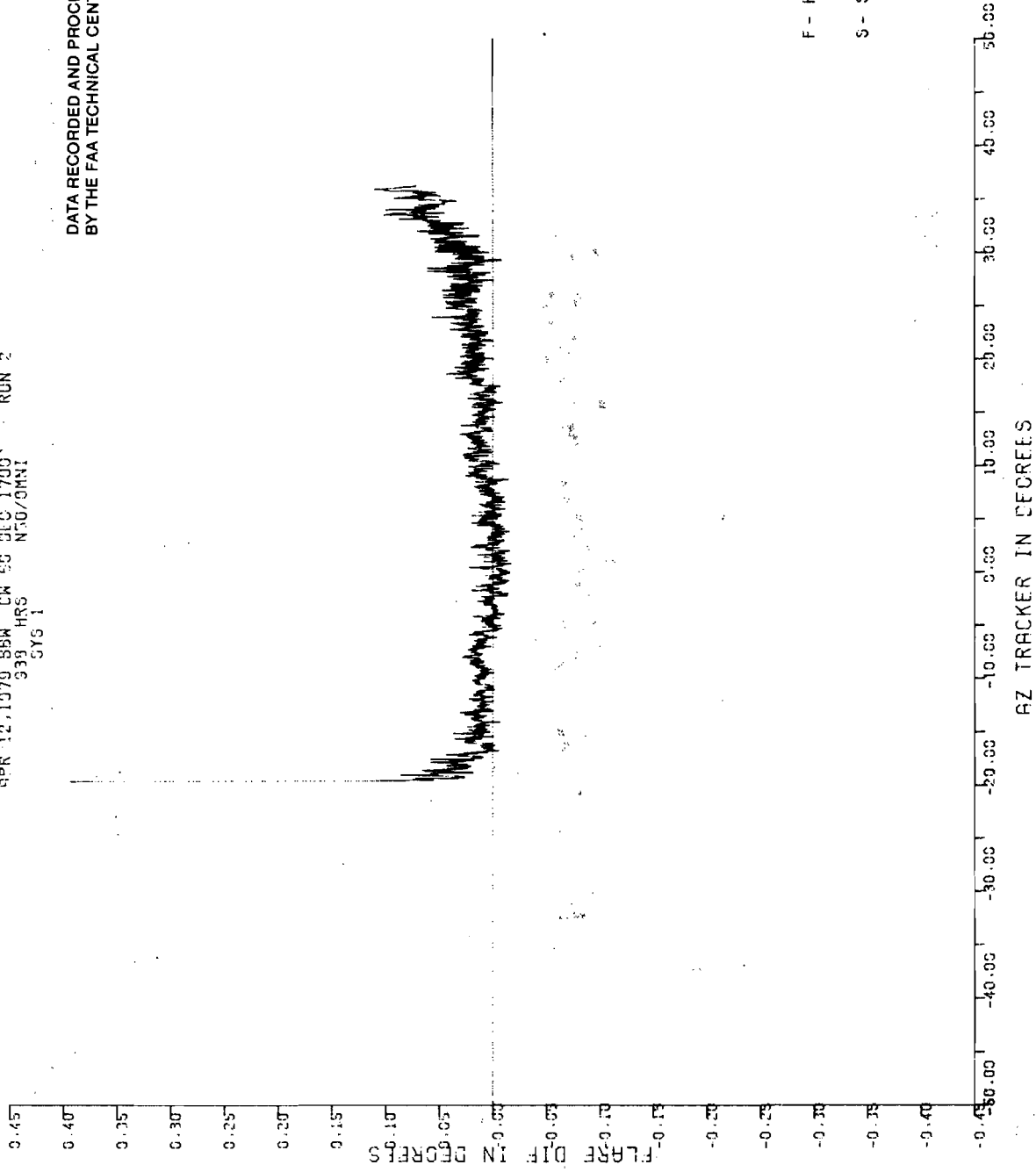
A-5

F - FRAME FLAG
S - SYSTEM FLAG

81-61-A-5

APR 12, 1979 854 CW 50 DEC 1700' RUN 2
939 HRS N30/0MNI
SYS 1

DATA RECORDED AND PROCESSED
BY THE FAA TECHNICAL CENTER

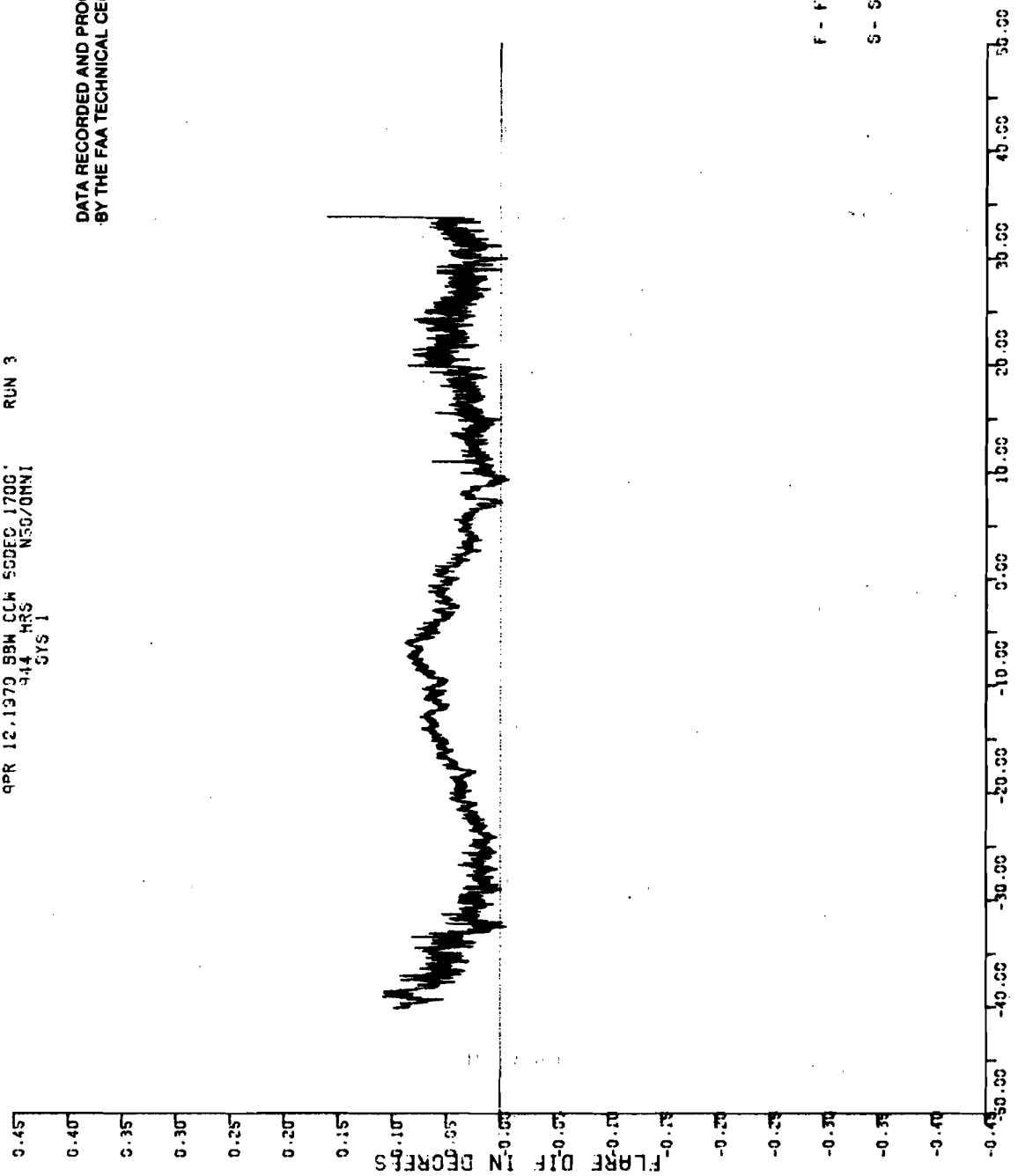


F - FRAME FLAG
S - SYSTEM FLAG

81-61-A-6

APR 12 1979 89M CCH 50DEC 1700' RUN 3
414 RRS NSG/ONMI
SYS 1

DATA RECORDED AND PROCESSED
BY THE FAA TECHNICAL CENTER



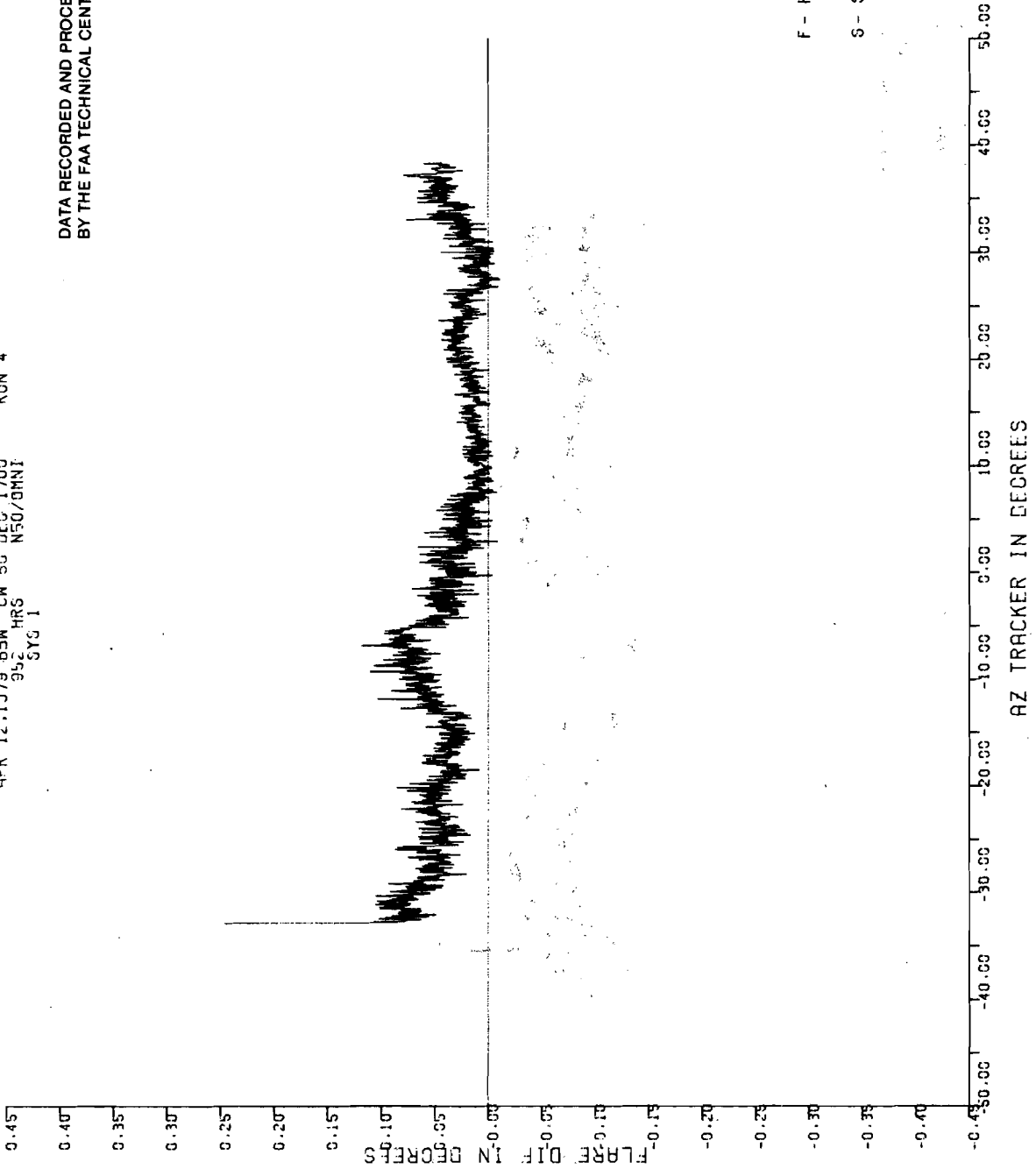
F - FRAME FLAG
S - SYSTEM FLAG

AZ TRACKER IN DEGREES

81-61-A-7

APR 12.1379.89W CM 50 DEC.1700.
9.5 HRS N50/08N1
SYS 1 RUN 4

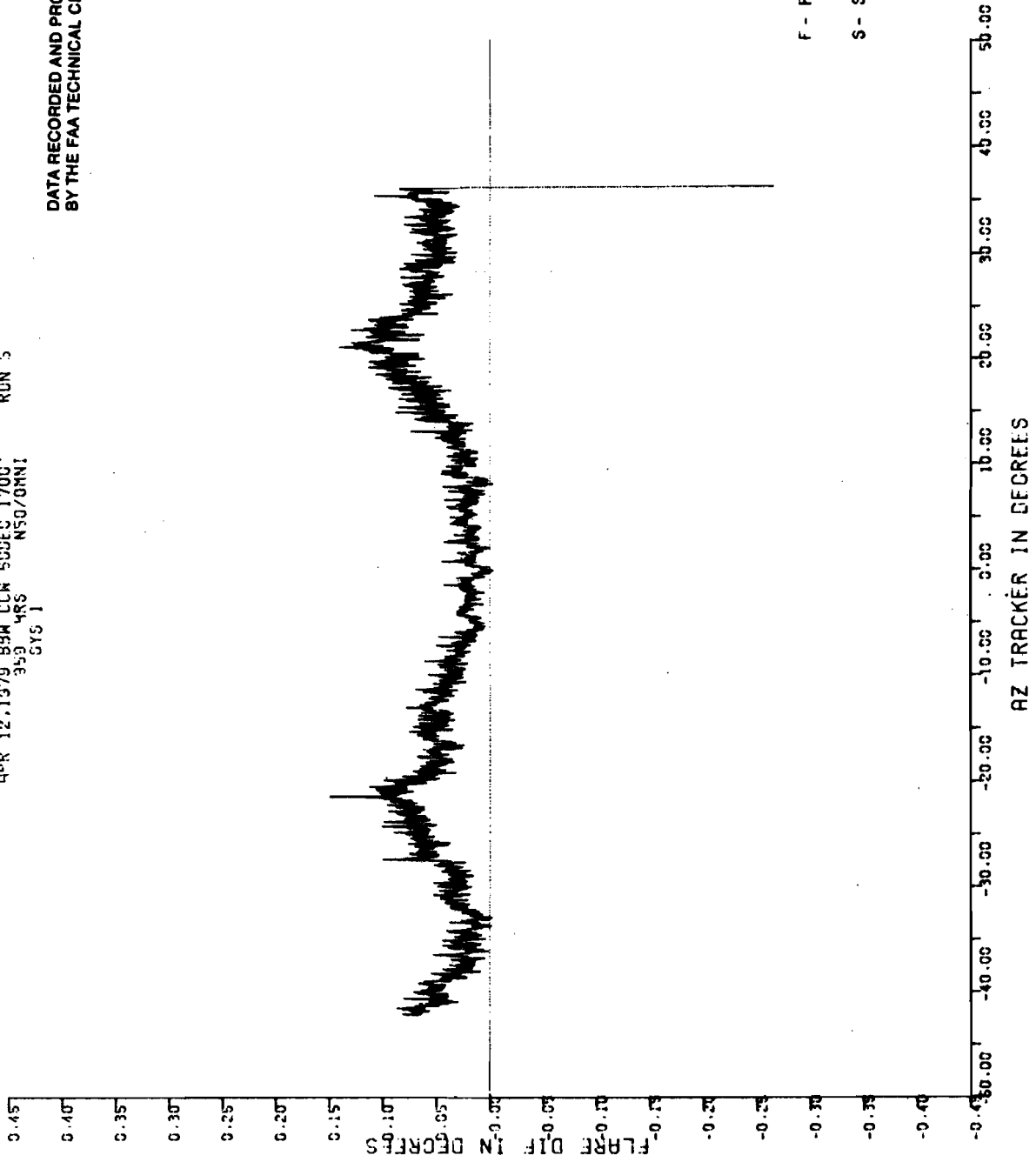
DATA RECORDED AND PROCESSED
BY THE FAA TECHNICAL CENTER



81-61-A-8

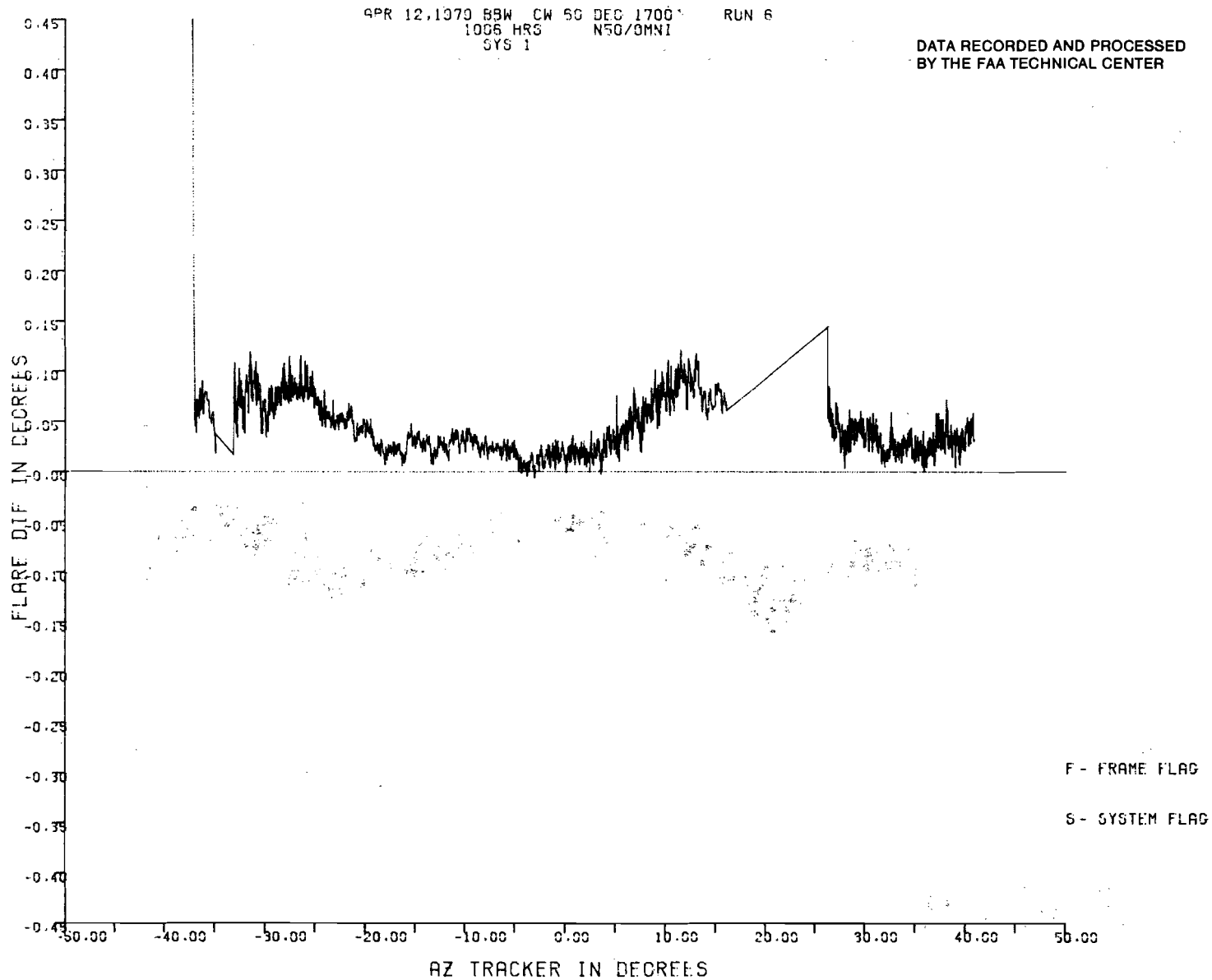
APR 12, 1979 59M CCM 50DEC 1700:
353 4RS
NSO/GNNI
SYS 1
RUN 5

DATA RECORDED AND PROCESSED
BY THE FAA TECHNICAL CENTER



81-61-A-9

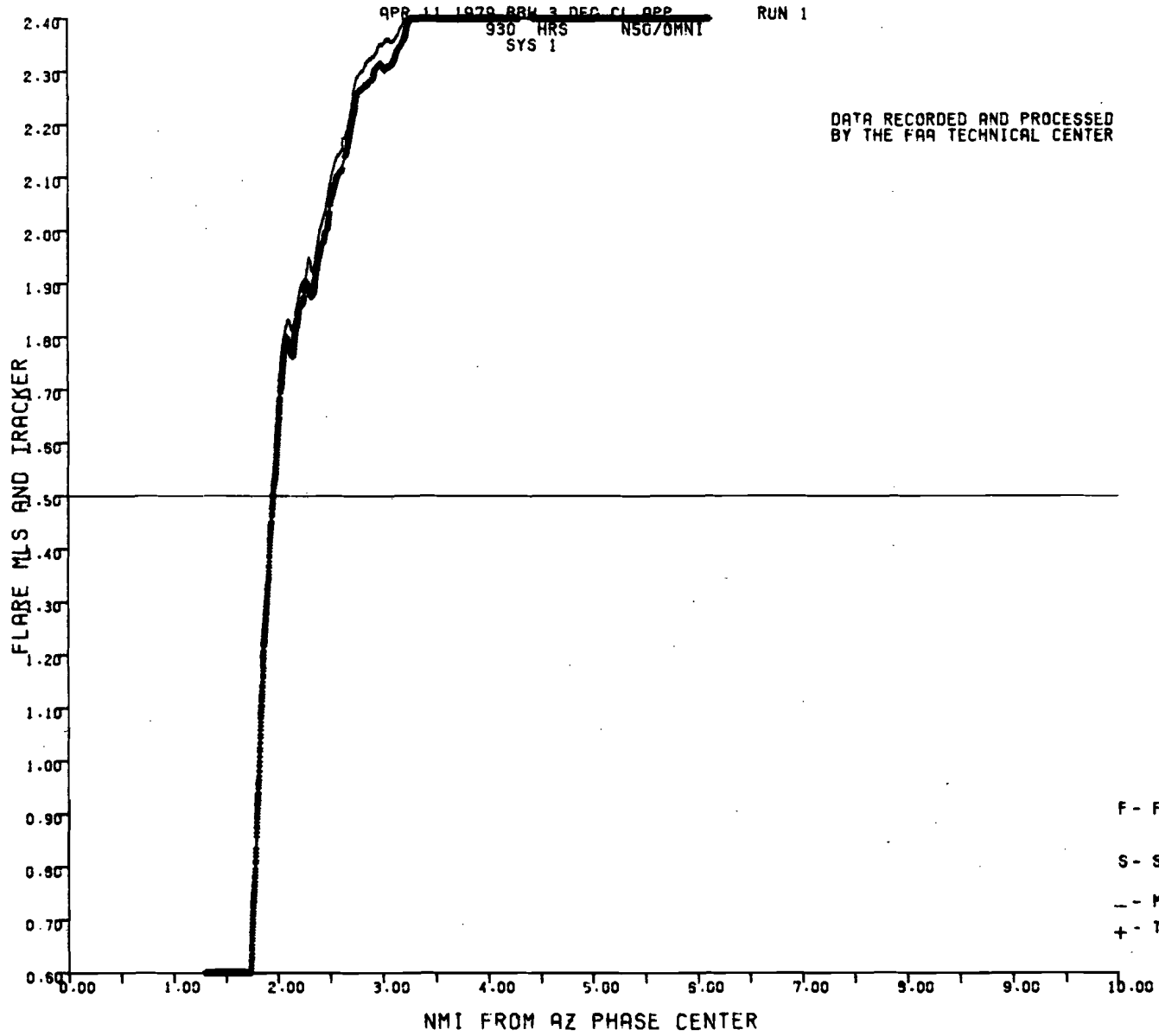
A-10



APPENDIX B
DIAGNOSTIC PLOTS

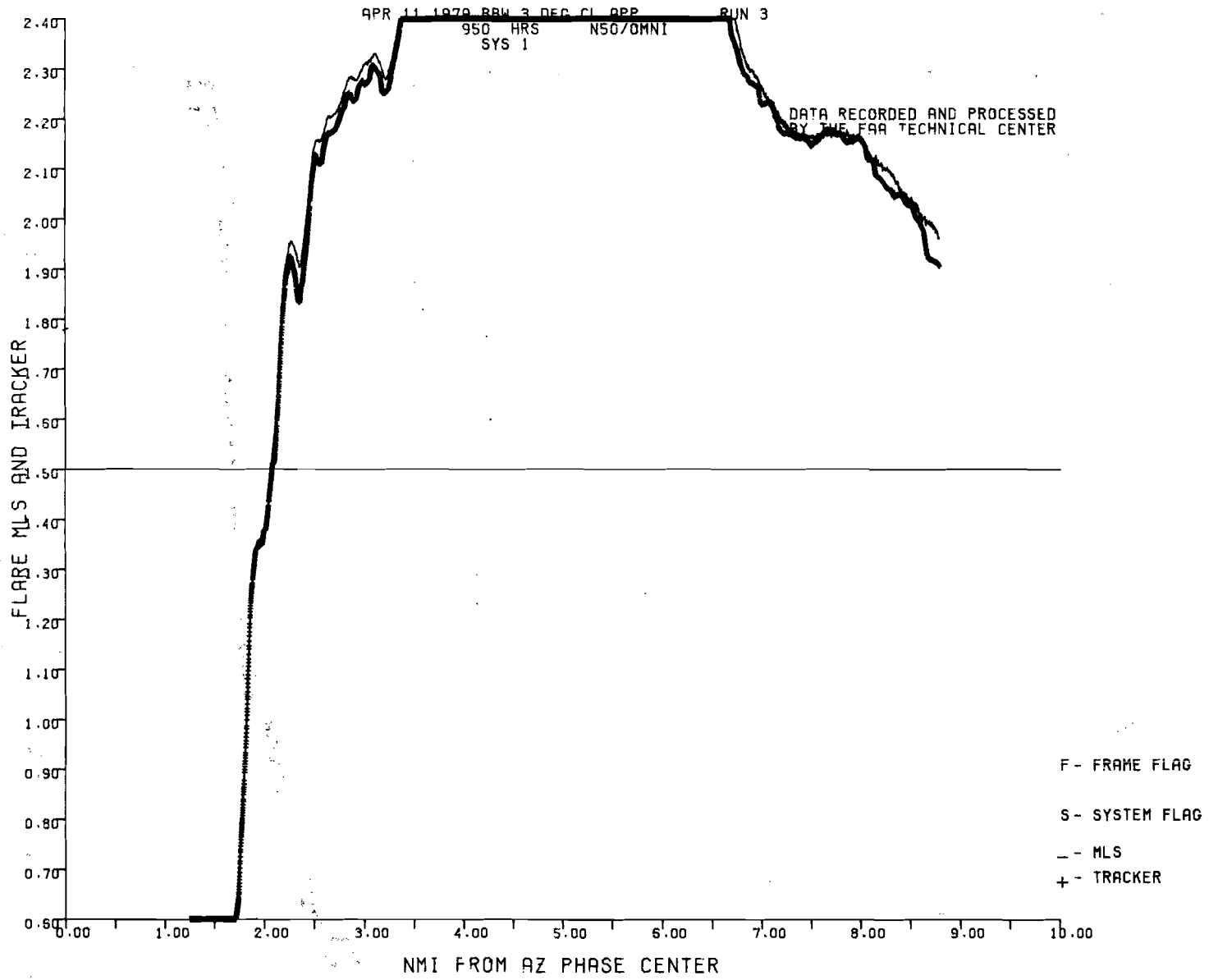
<u>Type of Pattern</u>	<u>Page No.</u>
Three degree glide slope, centerline	B-1 to B-5

B-1



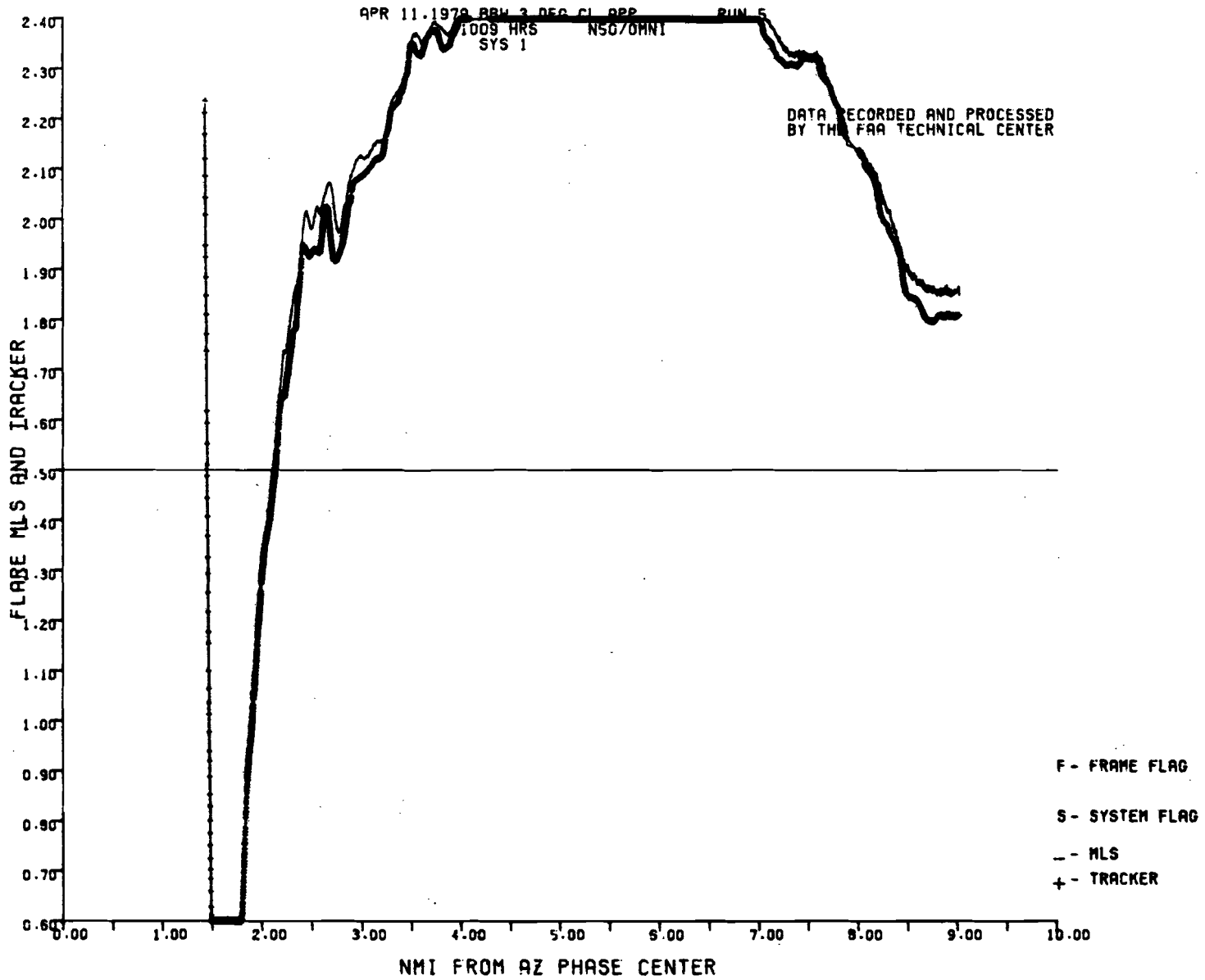
81-61-B-1

B-2

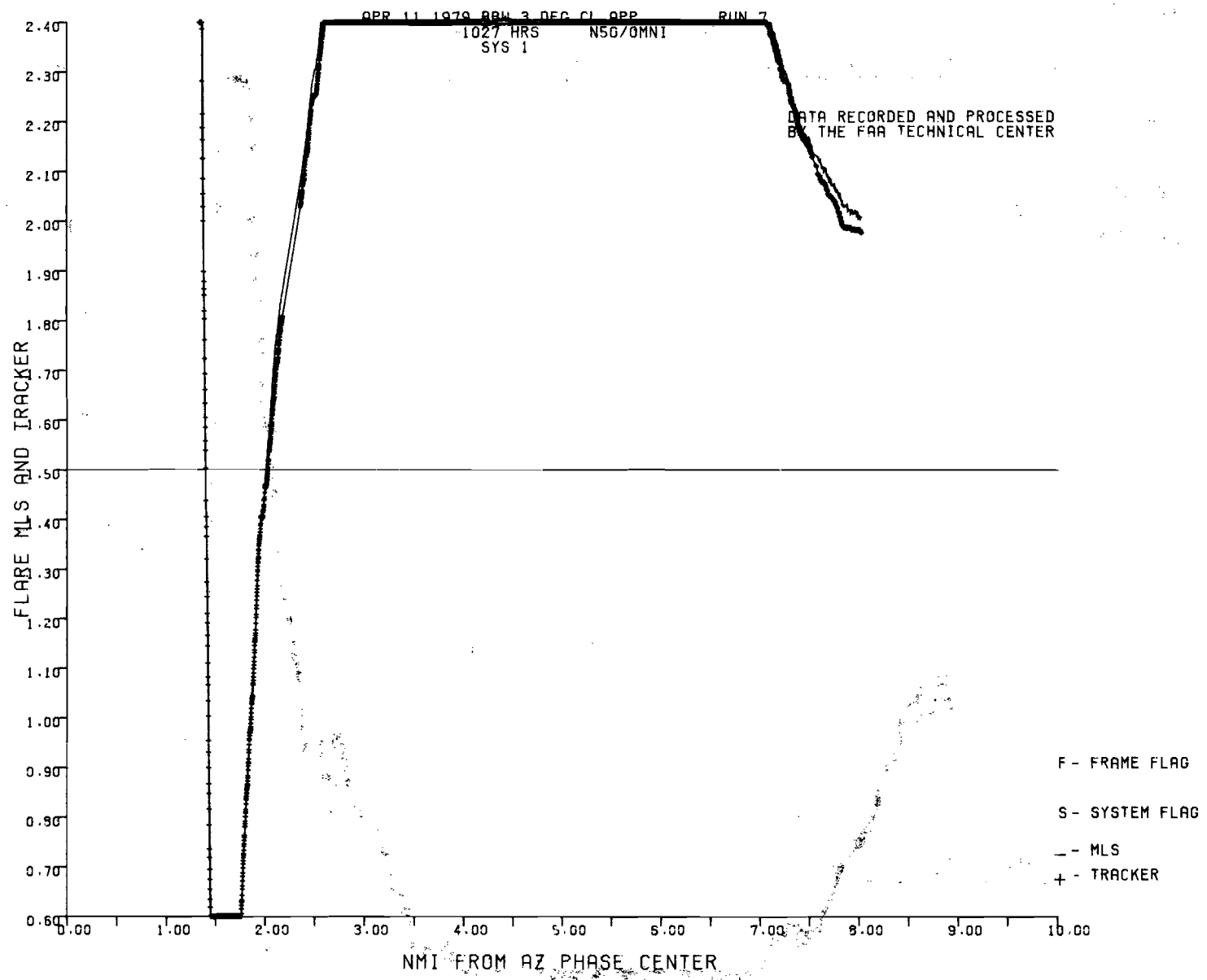


81-61-B-2

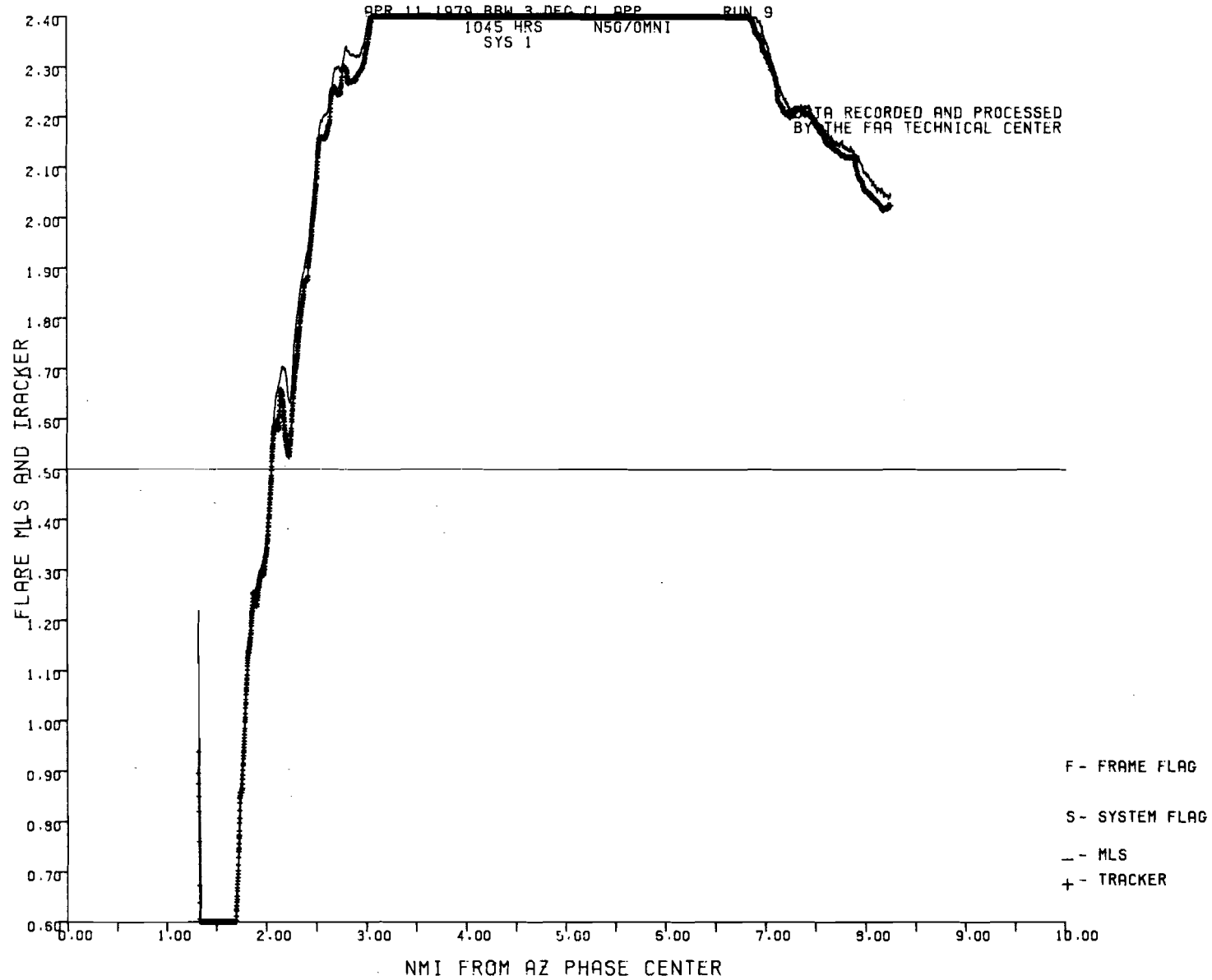
B-3



B-4



B-5



APPENDIX C

EXPANDED RAW AND PATH FOLLOWING ERROR PLOTS

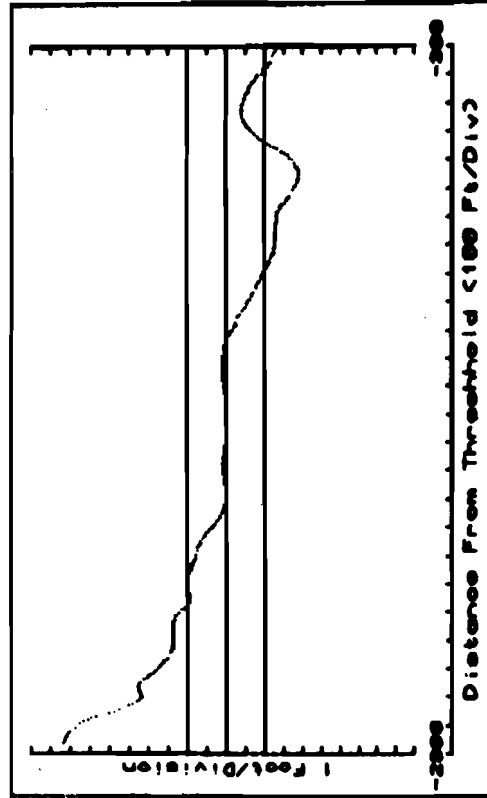
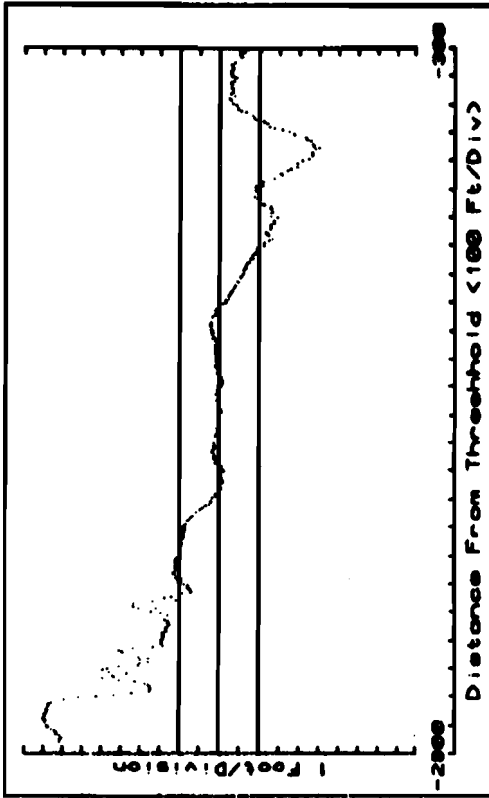
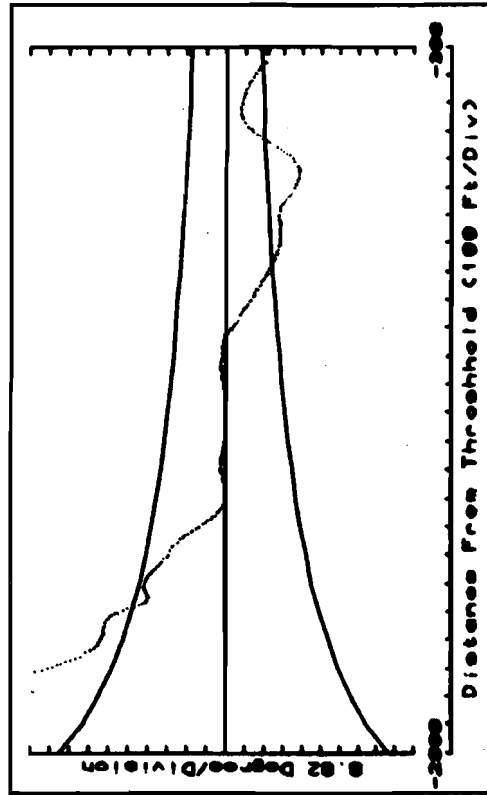
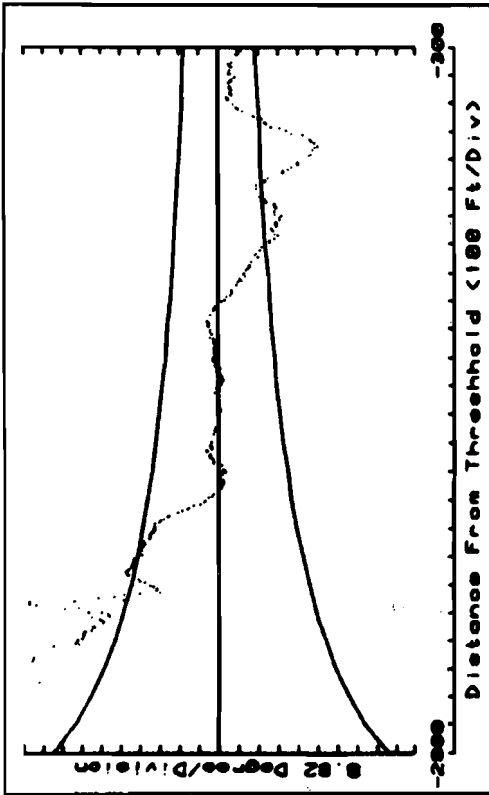
<u>Type of Pattern</u>	<u>Page No.</u>
Three degree glide slope, centerline	C-1 to C-5

MLS Flare Subsystem

11 April 1979 DATA RECORDED AND PROCESSED BY THE FAA TECHNICAL CENTER

Airborne Test Data

Run 1 Start Time 09:28:30

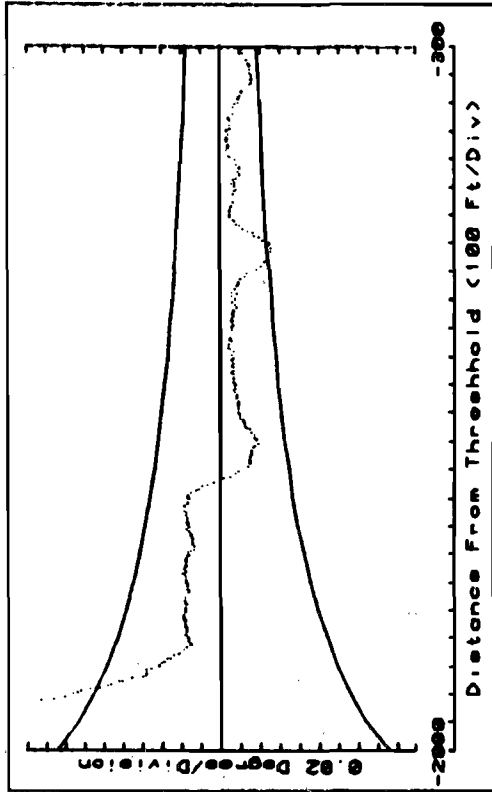


MLS Flare Subsystem

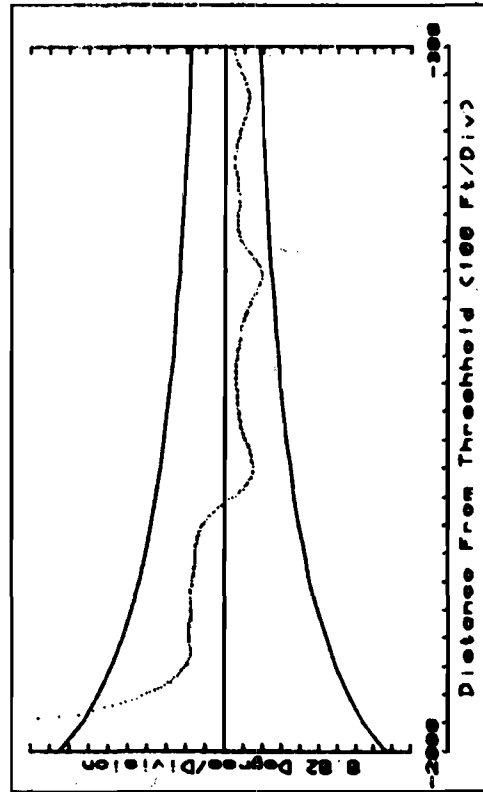
11 April 1979 DATA RECORDED AND PROCESSED BY THE FAA TECHNICAL CENTER

Airborne Test Data

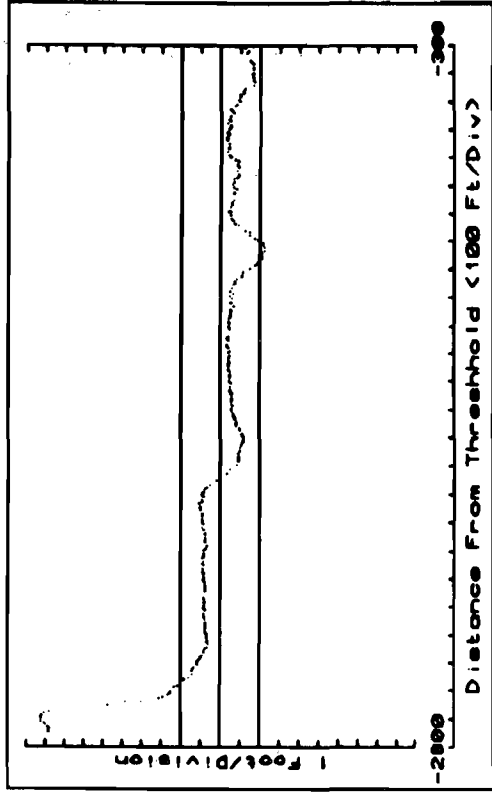
Run 3 Start Time 09:49:12



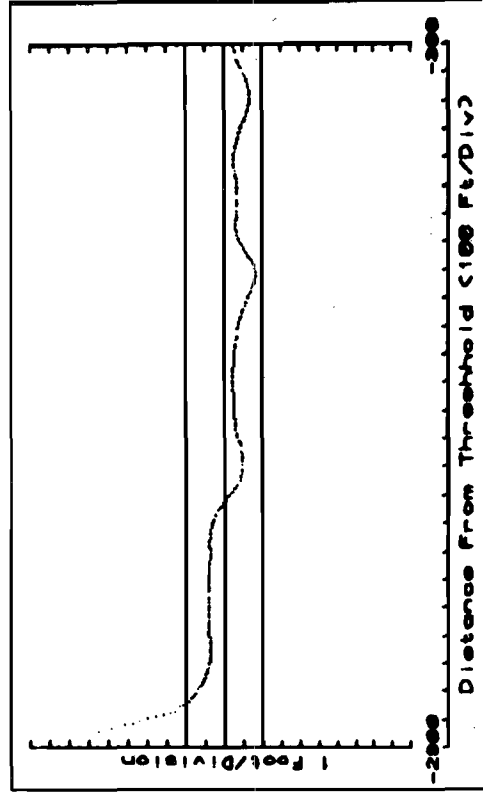
Raw Angular Error



PFE Filtered Angular Error



Raw Linear Error

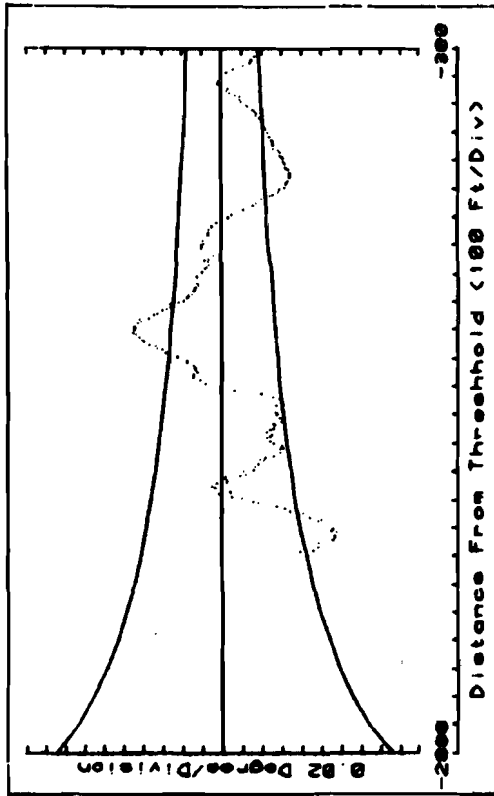


PFE Filtered Linear Error

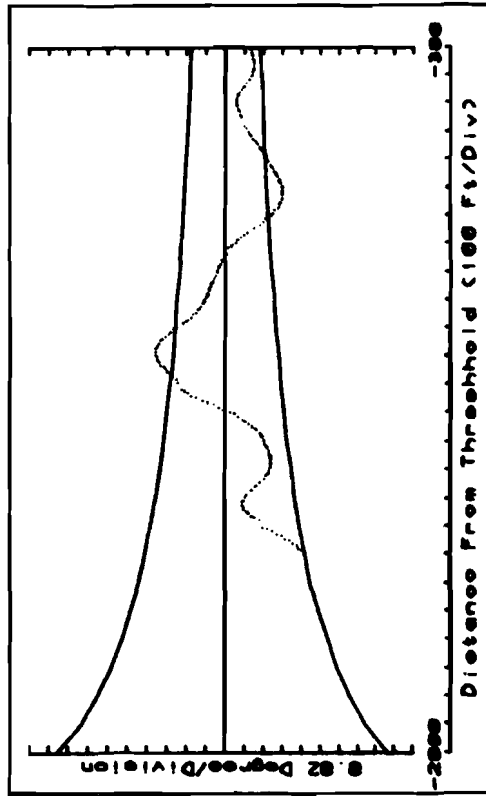
81-61-C-2

MLS Flare Subsystem
11 April 1979
DATA RECORDED AND PROCESSED
BY THE FAA TECHNICAL CENTER

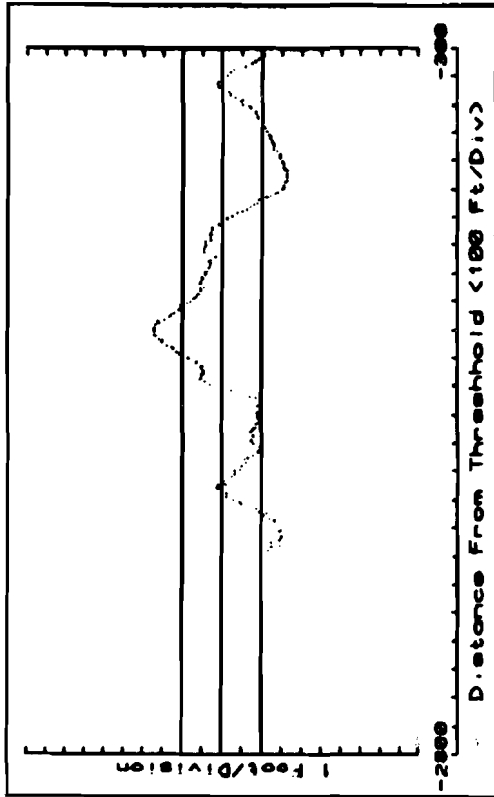
Airborne Test Data
Run 5 Start Time 10:09:05



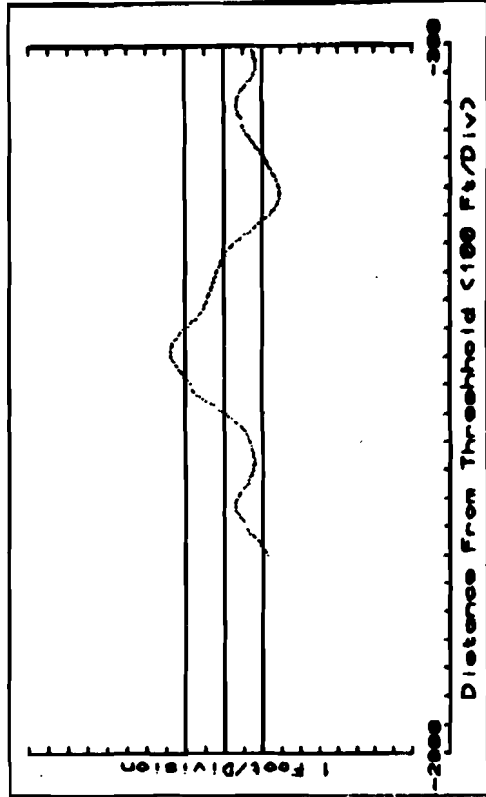
Raw Angular Error



PFE Filtered Angular Error



Raw Linear Error

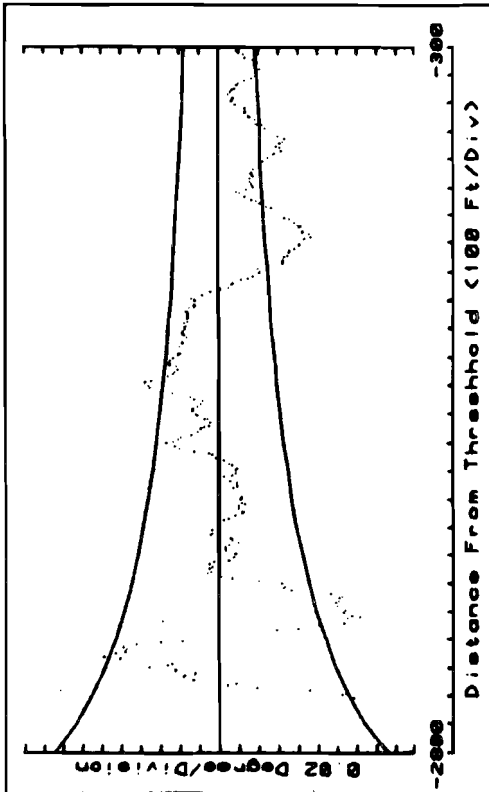


PFE Filtered Linear Error

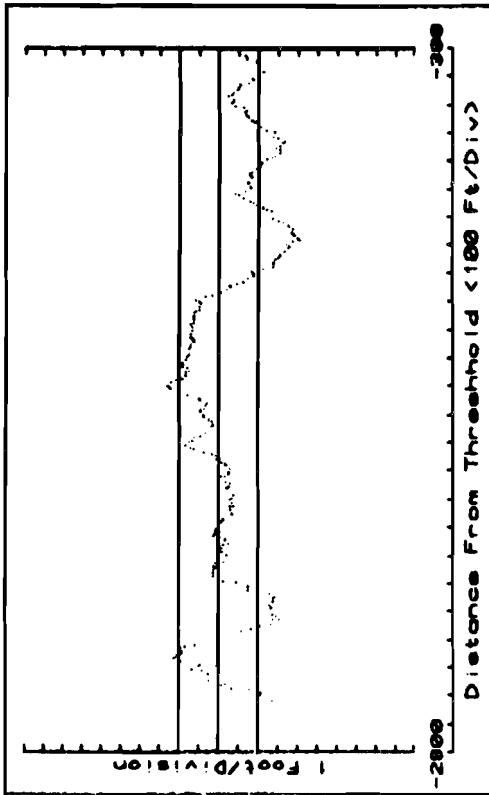
MLS Flare Subsystem Airborne Test Data

11 April 1979 Run 7 Start Time 10:27:17

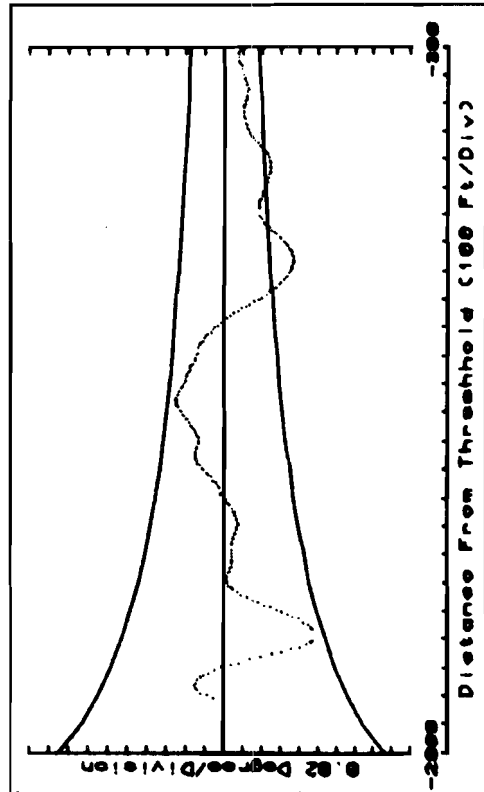
DATA RECORDED AND PROCESSED
BY THE FAA TECHNICAL CENTER



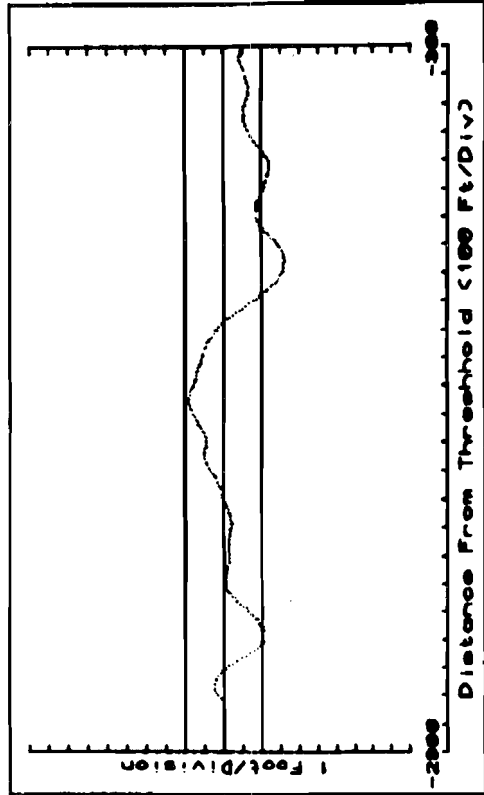
Raw Angular Error



Raw Linear Error



PFE Filtered Angular Error



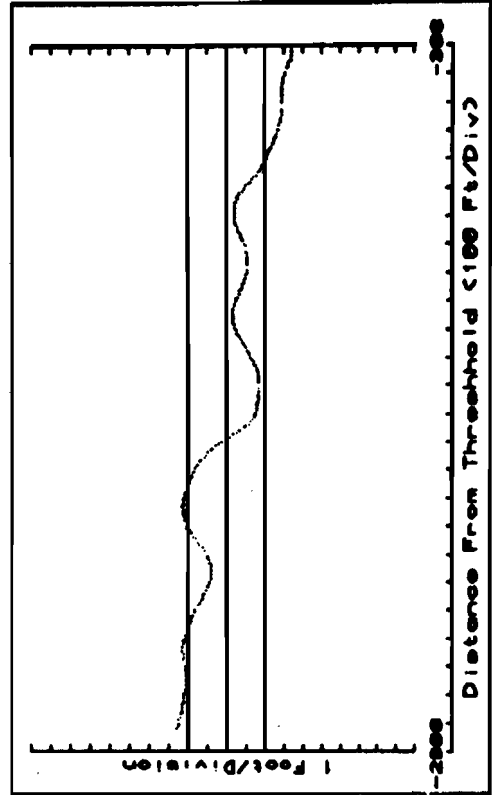
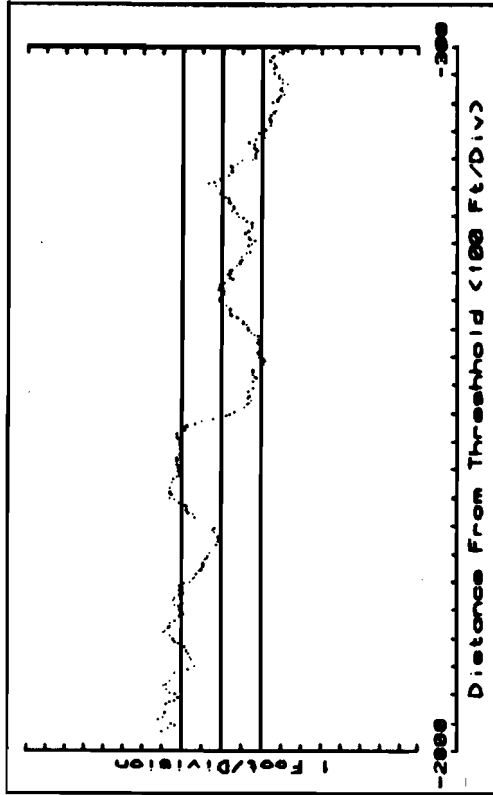
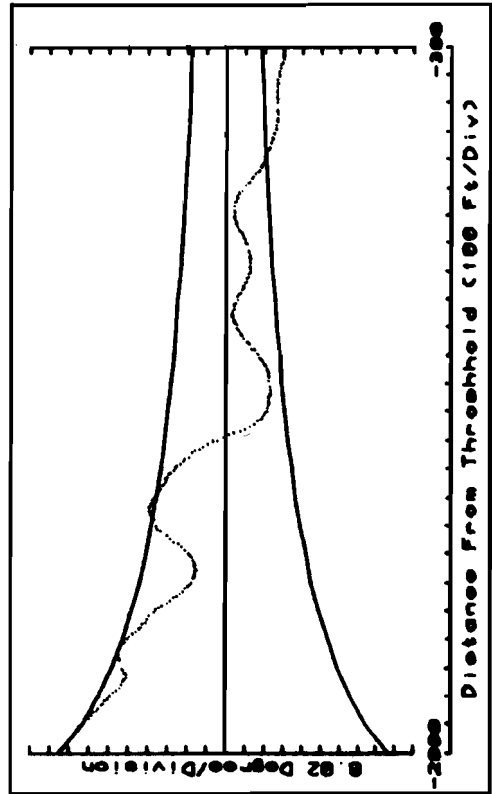
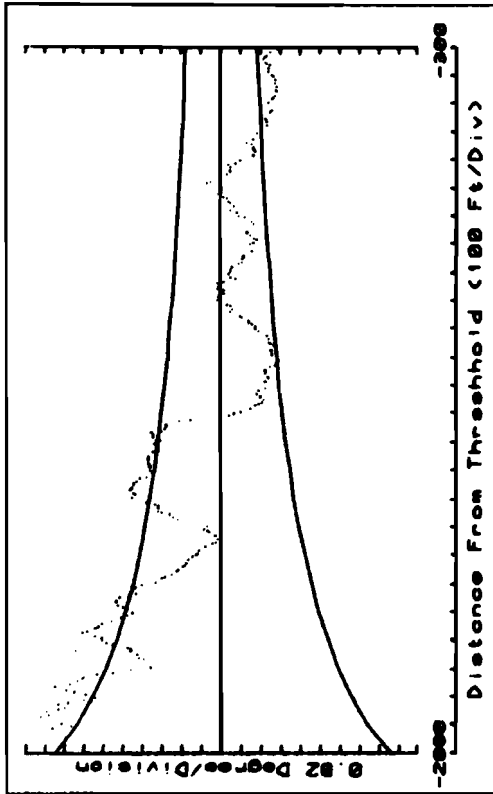
PFE Filtered Linear Error

MLS Flare Subsystem

11 April 1979 DATA RECORDED AND PROCESSED BY THE FAA TECHNICAL CENTER

Airborne Test Data

Run 9 Start Time 10:45:12



APPENDIX D

CONTROL MOTION NOISE PLOT

Type of Pattern

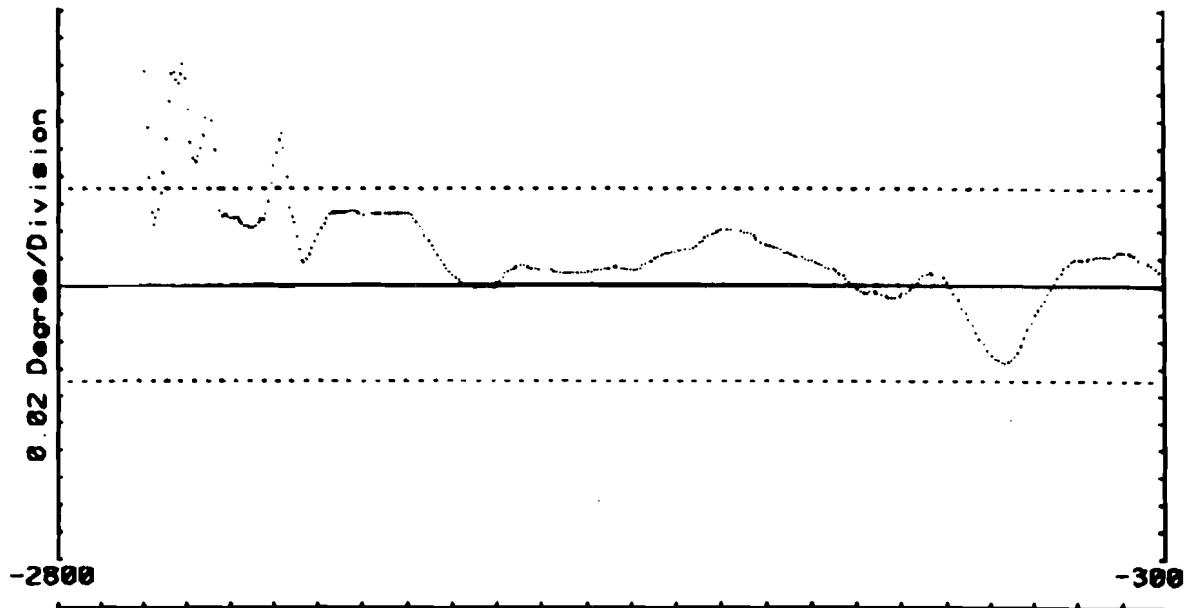
Page No.

Three degree glide slope, centerline

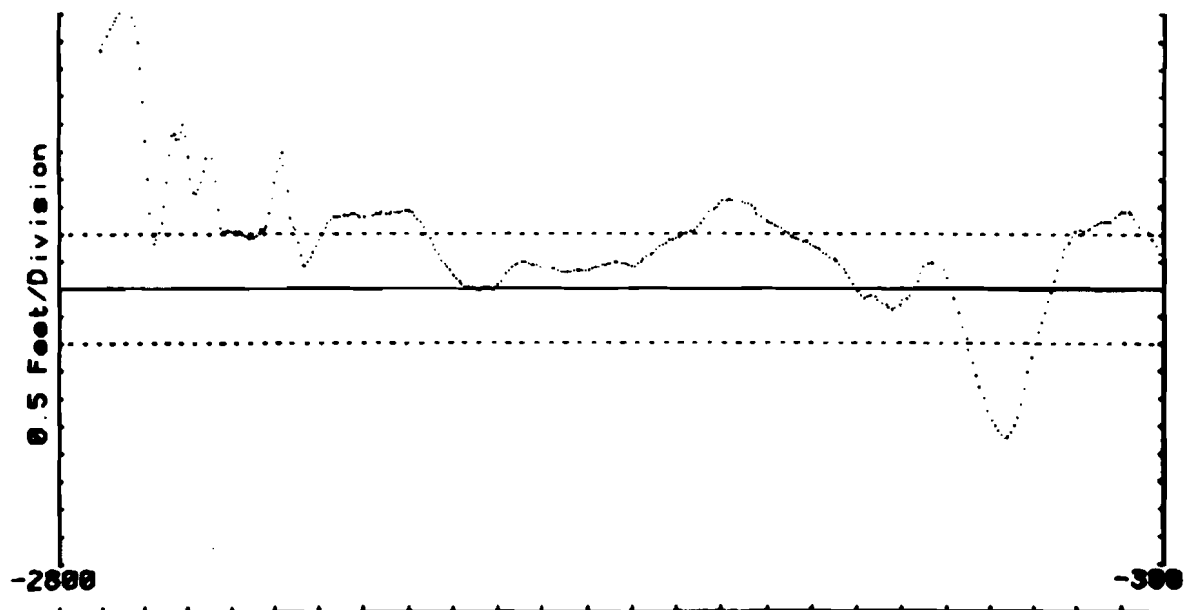
D-1 to D-5

MLS Flare Subsystem Airborne Test Data

11 April 1979 DATA RECORDED AND PROCESSED BY THE FAA TECHNICAL CENTER Run 1 Start Time 09:28:30



Distance From Threshold (100 Ft/Div)
Angular Control Motion Noise



Distance From Threshold (100 Ft/Div)
Linear Control Motion Noise

81-61-D-1

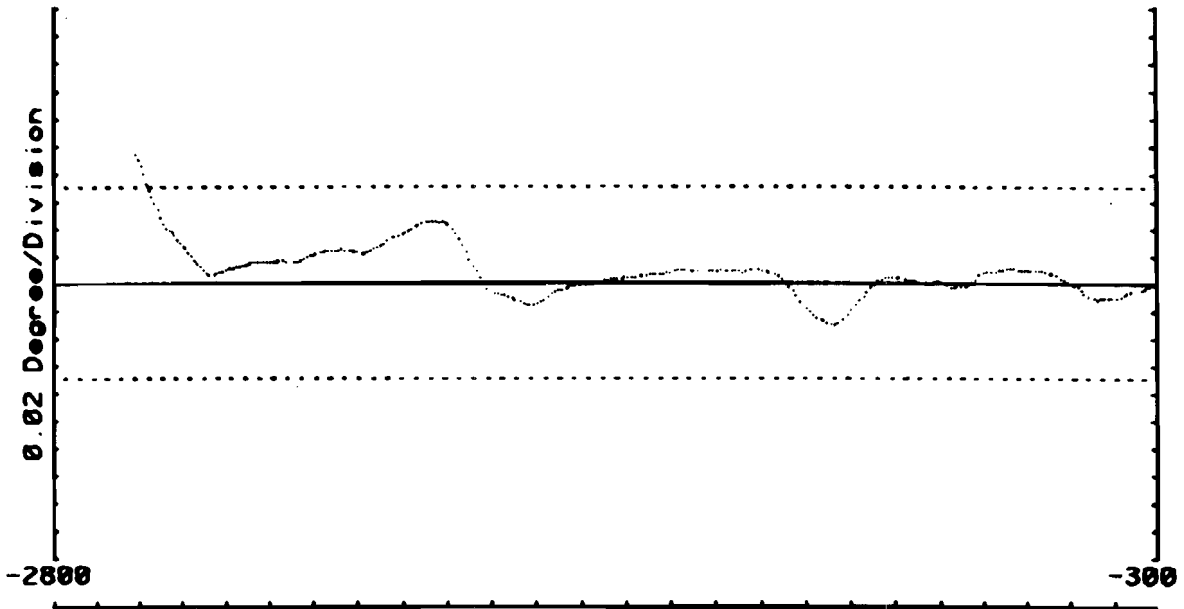
MLS Flare Subsystem Airborne Test Data

11 April 1979

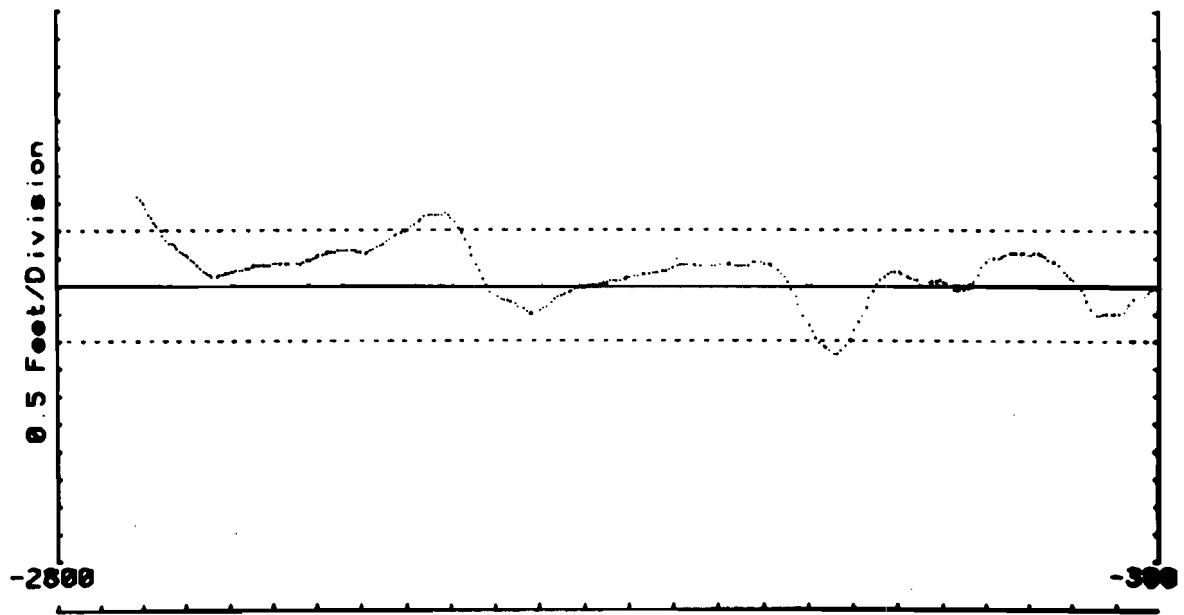
DATA RECORDED AND PROCESSED
BY THE FAA TECHNICAL CENTER

Run 3

Start Time 09:49:12



Distance From Threshold (100 Ft/Div)
Angular Control Motion Noise



Distance From Threshold (100 Ft/Div)
Linear Control Motion Noise

81-61-D-2

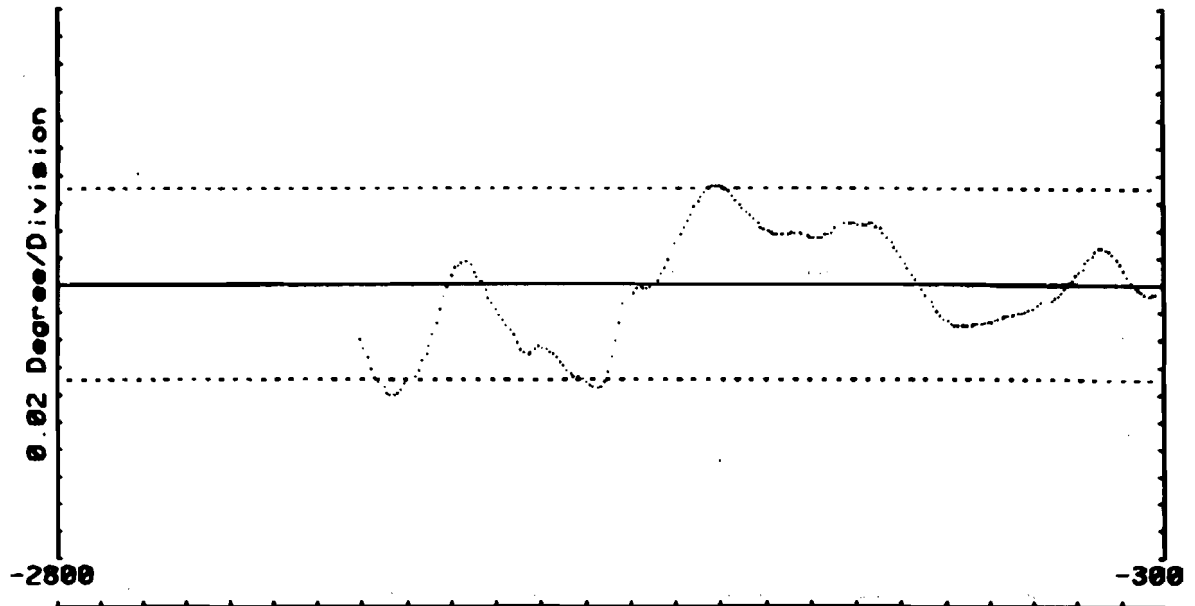
MLS Flare Subsystem Airborne Test Data

11 April 1979

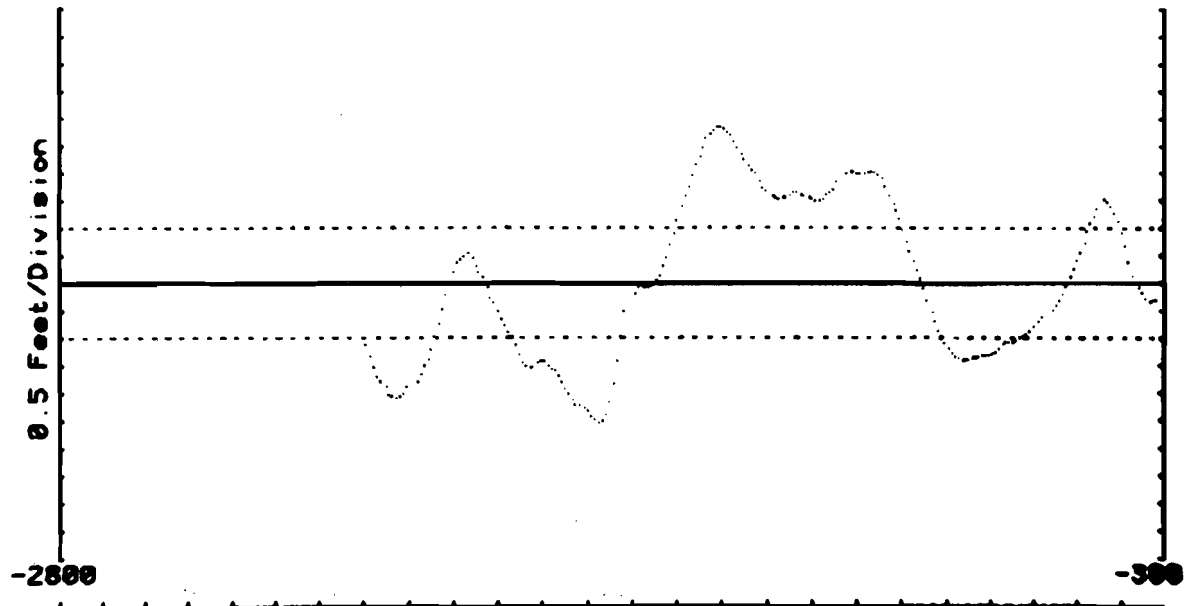
DATA RECORDED AND PROCESSED
BY THE FAA TECHNICAL CENTER

Run 5

Start Time 10:09:05



Distance From Threshold (100 Ft/Div)
Angular Control Motion Noise



Distance From Threshold (100 Ft/Div)
Linear Control Motion Noise

81-61-D-3

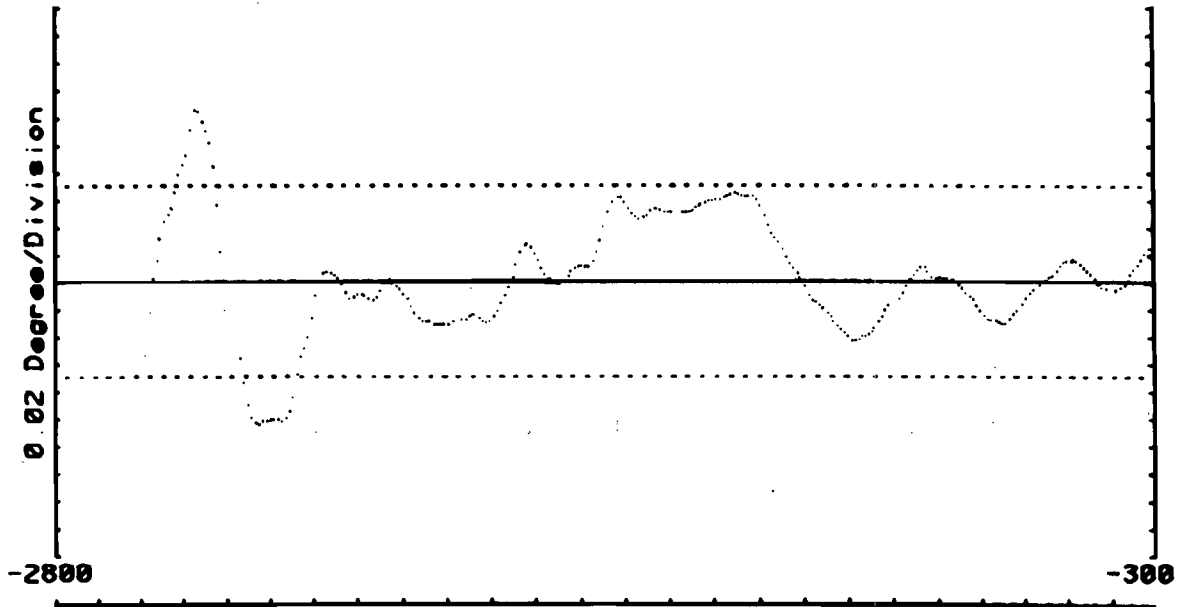
MLS Flare Subsystem Airborne Test Data

11 April 1979

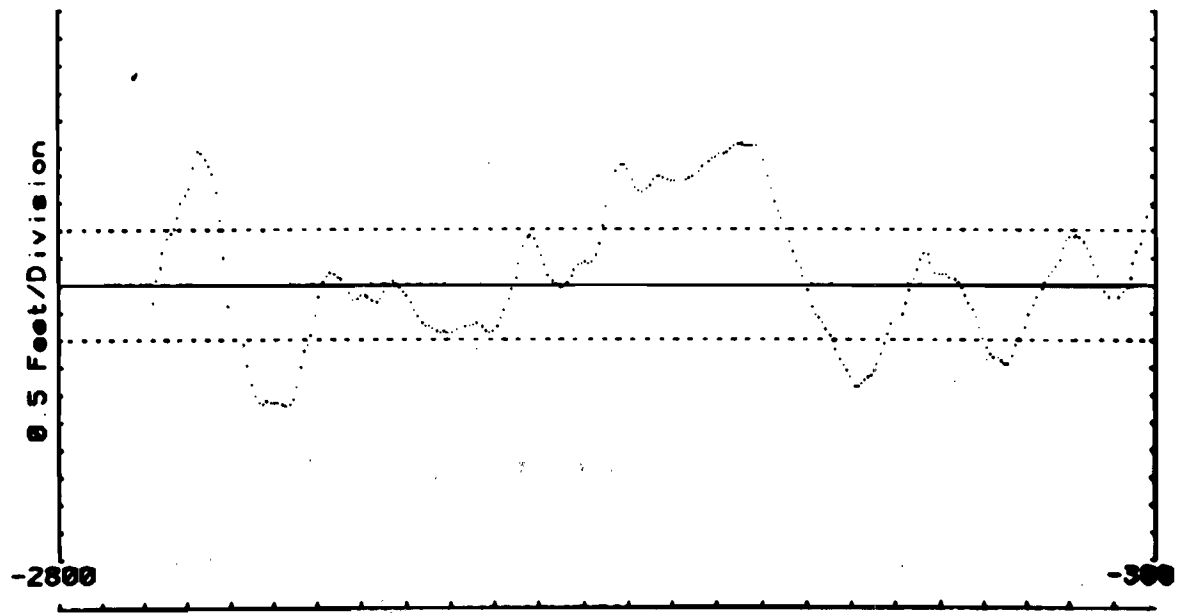
DATA RECORDED AND PROCESSED
BY THE FAA TECHNICAL CENTER

Run 7

Start Time 10:27:17



Distance From Threshold (100 Ft/Div)
Angular Control Motion Noise



Distance From Threshold (100 Ft/Div)
Linear Control Motion Noise

81-61-D-4

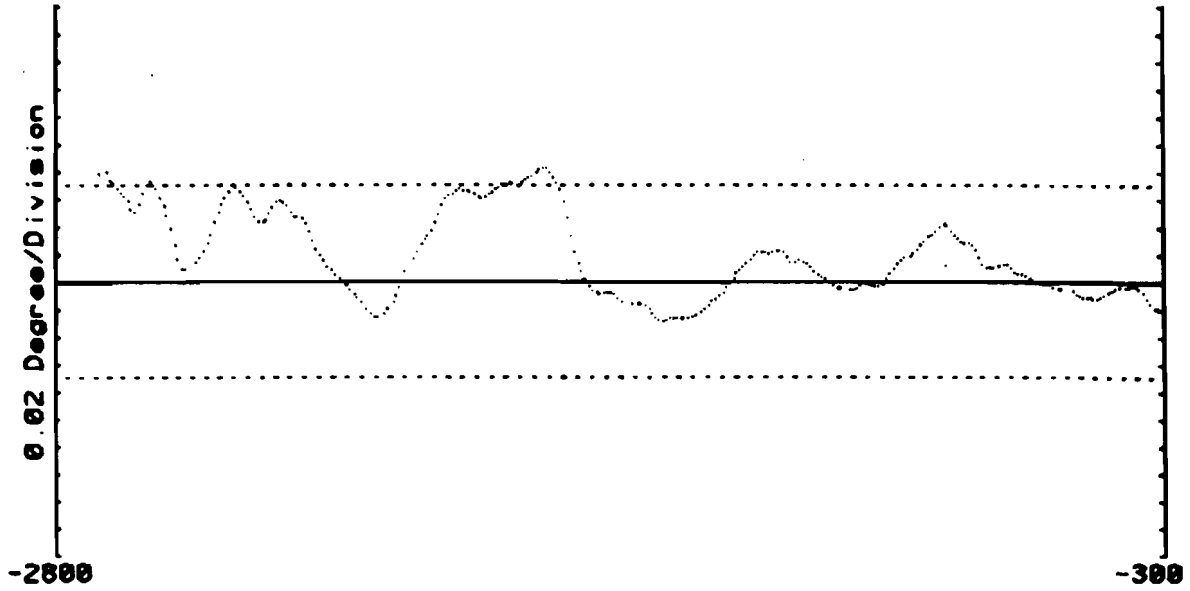
MLS Flare Subsystem Airborne Test Data

11 April 1979

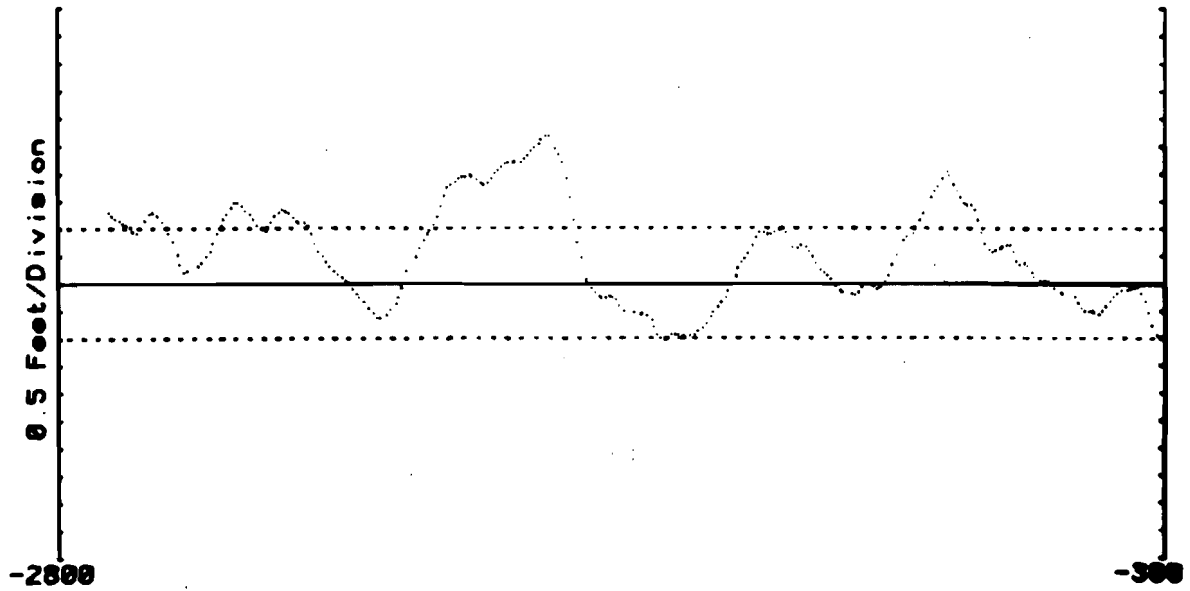
DATA RECORDED AND PROCESSED
BY THE FAA TECHNICAL CENTER

Run 9

Start Time 10:45:12



Distance From Threshold (100 Ft/Div)
Angular Control Motion Noise



Distance From Threshold (100 Ft/Div)
Linear Control Motion Noise

81-61-D-5